

NACA RM L54108



RESEARCH MEMORANDUM

FOR REFERENCE

NOT TO BE TAKEN FROM THIS ROOM

AERODYNAMIC CHARACTERISTICS OF VARIOUS CONFIGURATIONS

OF A MODEL OF A 45° SWEEP-WING AIRPLANE

AT A MACH NUMBER OF 2.01

By M. Leroy Spearman, Cornelius Driver,
and Ross B. Robinson

Langley Aeronautical Laboratory
Langley Field, Va.

LIBRARY COPY

MAY 31 1955

LANGLEY AERONAUTICAL LABORATORY
LIBRARY, NACA
LANGLEY FIELD, VIRGINIA

CLASSIFIED DOCUMENT

This material contains information affecting the National Defense of the United States within the meaning of the espionage laws, Title 18, U.S.C., Secs. 793 and 794, the transmission or revelation of which in any manner to an unauthorized person is prohibited by law.

NATIONAL ADVISORY COMMITTEE FOR AERONAUTICS

WASHINGTON

May 26, 1955

TO UNCLASSIFIED

CLASSIFICATION CHANGED

By Extension of DASA CCLP H430 on 12-29-65

Kind 1-24-65

UNCLASSIFIED

NASA Technical Library



3 1176 01437 1794

NACA RM L54J08

~~CONFIDENTIAL~~

NATIONAL ADVISORY COMMITTEE FOR AERONAUTICS

RESEARCH MEMORANDUM

AERODYNAMIC CHARACTERISTICS OF VARIOUS CONFIGURATIONS

OF A MODEL OF A 45° SWEEP-WING AIRPLANE

AT A MACH NUMBER OF 2.01

By M. Leroy Spearman, Cornelius Driver,
and Ross B. Robinson

SUMMARY

An investigation has been conducted in the Langley 4- by 4-foot supersonic pressure tunnel at a Mach number of 2.01 to determine the aerodynamic characteristics of several configurations of a model of a 45° swept-wing airplane. The basic configuration had a wing with 45° sweepback at the quarter-chord line, aspect ratio 3.2, taper ratio 0.468, NACA 65A005.5 sections just outboard of the inlet, and NACA 65A003.7 sections at the tip. The wing was mounted slightly above the body center line and an all-movable horizontal tail was located slightly below the extended chord line of the wing. The design incorporated twin wing-root supersonic inlets ducted to a single exit at the base of the fuselage. The configurations investigated included an extended nose length, a bumped-fuselage afterbody, an inlet droop, an increased wing aspect ratio, and a revised canopy shape.

Configurations employing the wing of increased aspect ratio of 3.7, which constituted the bulk of the tests, produced about a 10-percent increase in lift and in longitudinal stability as compared with the basic wing of aspect ratio 3.2. There was a slight but measurable increase in minimum drag and maximum lift-drag ratio.

For the basic configuration with the modified wing of aspect ratio 3.7, the maximum horizontal tail deflection of -16° resulted in a trim lift coefficient of about 0.3 at an angle of attack of 7.7° , a trim drag coefficient of 0.086, and a trim lift-drag ratio of 3.5. An effective upwash at the low horizontal tail contributed to the high degree of longitudinal stability. The minimum trim drag coefficient for a horizontal tail deflection of -3° was about 0.035.

~~CONFIDENTIAL~~

UNCLASSIFIED

The basic configuration with the modified wing of aspect ratio 3.7 indicated positive directional and lateral stability at zero angle of attack (slight negative lift). The addition of a longer nose to the body had a negligible effect on the lift, drag, and longitudinal stability but reduced the directional stability so that instability might occur with increasing angle of attack. The addition of the bump to the fuselage afterbody apparently resulted in a slight reduction in minimum drag although the difference was within the accuracy of the drag measurements.

INTRODUCTION

An investigation of the aerodynamic characteristics in pitch and sideslip at a Mach number of 2.01 of a model of a 45° swept-wing fighter-type airplane configuration has been conducted in the Langley 4- by 4-foot supersonic pressure tunnel. During the course of the investigation, various modifications were made to the model to determine their effects upon its aerodynamic characteristics. These modifications included a lengthened body nose, a faired bump on the fuselage afterbody designed to improve the longitudinal area distribution, drooped inlets, and an extension to the wing tips that resulted in an increase in the aspect ratio of the wing from 3.2 to 3.7. Because of the paucity of data on such modifications in the supersonic speed range it was thought that the results would be of considerable general interest.

SYMBOLS

All coefficients are based upon the geometry of the basic wing of aspect ratio 3.2. The force and moment coefficients are referred to the stability-axis system with the reference center-of-gravity location (center of moments) at the 25-percent-chord point of the basic-wing mean aerodynamic chord.

A	aspect ratio
C_L	lift coefficient, $\frac{-Z}{qS}$
C_D'	external-drag coefficient, $\frac{-X}{qS}$

C_m	pitching-moment coefficient, $\frac{M'}{qS\bar{c}}$
C_Y	side-force coefficient, $\frac{Y}{qS}$
C_l	rolling-moment coefficient, $\frac{L'}{qSb}$
$C_{l_\beta} = \frac{\partial C_l}{\partial \beta}$	per deg
C_n	yawing-moment coefficient, $\frac{N}{qSb}$
$C_{n_\beta} = \frac{\partial C_n}{\partial \beta}$	per deg
Z	force along stability Z-axis
X	force along stability X-axis
M'	moment about stability Y-axis
Y	force along stability Y-axis
L'	moment about stability X-axis
N	moment about stability Z-axis
S	area of basic wing of aspect ratio 3.2 obtained by extending leading and trailing edges to body center line (neglecting inlet outline)
b	span of basic wing
c	chord, ft
\bar{c}	mean aerodynamic chord of basic wing
q	dynamic pressure
M	free-stream Mach number

L/D	lift-drag ratio, C_L/C_D'
α	angle of attack, deg
β	angle of sideslip, deg
i_t	angle of incidence of horizontal tail, deg
ϵ	effective downwash angle, deg

MODEL AND APPARATUS

The tests were conducted in the Langley 4- by 4-foot supersonic pressure tunnel at a Mach number of 2.01. A three-view drawing of the model of a 45° swept-wing airplane is shown in figure 1 and its geometric characteristics are presented in table I. The longitudinal area distribution of the basic model and the model with a bumped afterbody is shown in figure 2. Photographs of the model are shown as figure 3.

The basic configuration had a wing with 45° sweepback at the quarter-chord line, an NACA 65A005.5 section just outboard of the inlet ($.38b/2$), and an NACA 65A003.7 section at the tip. The basic wing had a taper ratio of 0.468, an aspect ratio of 3.2, a geometric dihedral angle of -3.5° , and was located slightly above the fuselage center line. An all-movable horizontal tail was mounted below the extended chord plane of the wing.

The model was equipped with twin wing-root supersonic inlets ducted to a single exit at the base of the fuselage. The duct system incorporated a boundary-layer diverter with a wedge half angle of 49° . All tests were made with air flow through the ducts. The total pressure and static pressure at the duct exit were determined through the use of a rake mounted on the sting support rearward of the duct exit.

Tests were made of various modifications to the basic configuration. These modifications included a lengthened body nose (fig. 1); a bumped fairing on the fuselage afterbody designed to reduce the rise in the drag coefficient at transonic speeds by improving the longitudinal area distribution (figs. 1 and 2); extended wing tips that resulted in an increase in the aspect ratio from 3.2 to 3.7 (fig. 1); a 5° droop to that portion of the inlet ahead of the leading edge of the wing (fig. 3(a)); and two transition fairings or fillets at the juncture between the leading edge of the wing and the inlet (figs. 1 and 3(e)). The fillet faired smoothly into the leading edge of the wing (corresponding to a 0° leading-edge

flap position), and the other fillet extended below the leading edge of the wing in a position so that the inlet would fair smoothly into a $7\frac{1}{2}^{\circ}$ deflected leading-edge flap. In addition to these modifications, a flat-front canopy was tested in place of the vee-front canopy (figs. 1 and 3(d)) used for all other tests.

Forces and moments were measured by means of a six-component internal strain-gage balance.

TESTS

Test Conditions and Procedure

The tests were made at a Mach number of 2.01, a stagnation pressure of 13 pounds per square inch absolute, and a stagnation temperature of 100° F. The dewpoint was maintained sufficiently low (below -25°) so that no significant condensation effects were encountered.

The Reynolds number based on a mean aerodynamic chord of 0.522 foot was 1.673×10^6 . The dynamic pressure for the tests was about 663 pounds per square foot.

The angle of attack was varied from about -4° to 15° at zero sideslip; the angle of sideslip varied from about -4° to 9° at zero angle of attack.

Corrections and Accuracy

The angles of attack and sideslip have been corrected for deflections of the balance and the sting under load.

Base pressure measurements were made and the drag coefficients were adjusted to correspond to free-stream static pressure at the base. The internal pressure of the model was measured and corrections for a buoyant force on the balance have been applied to the drag results. The internal drag was determined from the change in momentum from free-stream conditions to the measured conditions at the duct exit. The base drag, buoyant force, and internal drag have been subtracted from the total drag measurements so that a net external drag was obtained. The mass-flow ratio was about 0.87 for all tests.

The estimated errors in the individual measured quantities are as follows:

C_L	± 0.0013
$C_{D'}$	± 0.0013
C_m	± 0.0003
C_z	± 0.0005
C_n	± 0.0002
C_Y	± 0.0002
α , deg	± 0.1
β , deg	± 0.1
i_t , deg	± 0.1
M	± 0.01

PRESENTATION OF RESULTS

The results are presented in the following manner:

	Figure
Effect of horizontal tail on aerodynamic characteristics in pitch. Basic nose; bump off; $A = 3.7$; undrooped inlet	4
Longitudinal characteristics for trim, $C_m = 0$. Basic nose; bump off; $A = 3.7$; undrooped inlet	5
Pitching effectiveness and effective downwash characteristics of the tail. Basic nose; bump off; $A = 3.7$; undrooped inlet	6
Effect of nose length and body bump on aerodynamic characteristics in pitch. $A = 3.7$; undrooped inlet; $i_t = -3^\circ$	7
Effect of nose length and body bump on aerodynamic characteristics in sideslip. $A = 3.7$; undrooped inlet; $\alpha = 0^\circ$; $i_t = -3^\circ$	8
Aerodynamic characteristics in sideslip. Basic nose; bump off; undrooped inlet; $A = 3.7$; $\alpha = 0^\circ$	9
Effect of inlet droop on aerodynamic characteristics in pitch. Basic nose; bump off; $A = 3.7$; $i_t = -3^\circ$	10
Effect of aspect ratio on aerodynamic characteristics in pitch. Basic nose; bump off; drooped inlet with 0° fairing; $i_t = -3^\circ$	11
Effect of canopy shape and horizontal tail deflection on aerodynamic characteristics in pitch. Basic nose; bump off; drooped inlet with 0° fairing; $A = 3.2$	12

Figure

Effect of inlet transition fairing on aerodynamic characteristics in pitch. Basic nose; bump off;

$A = 3.2$; $i_t = -3^\circ$ 13

DISCUSSION

Longitudinal stability and control of model with basic nose, bump off, undrooped inlet, and with aspect ratio, 3.7.- The aerodynamic characteristics in pitch for the configuration with various horizontal tail settings as well as with the horizontal tail removed (fig. 4) have been used to determine the longitudinal characteristics for trim (fig. 5). These results indicate a reasonably linear variation of angle of attack and horizontal-tail incidence with trim lift coefficient. The minimum trim drag coefficient is about 0.035 for a horizontal tail deflection of -3° and a trim lift coefficient of 0.054. The usefulness of the trim results (fig. 5) in determining the performance and maneuverability characteristics for a constant Mach number of 2.01 is obviously limited to that portion of the curves wherein the available engine thrust would be sufficient to overcome the drag produced. However, disregarding thrust availability, the results indicate that for the maximum horizontal tail deflection investigated (-16°) a trim lift coefficient of about 0.3 would be obtained at an angle of attack of about 7.7° with a drag coefficient of 0.086 and a lift-drag ratio of 3.5.

The pitching effectiveness of the tail (variation of pitching-moment coefficient with horizontal-tail deflection $\partial C_m / \partial i_t$) at $\alpha = 0^\circ$ (fig. 6(a)) indicates a value of about -0.0106. The variation of effective downwash with angle of attack (fig. 6(b)) as obtained from the tail-on and tail-off results from figure 4 indicates a negative value of $\partial \epsilon / \partial \alpha$ or an effective upwash at the tail that probably results from the upwash field of the body. The unpublished results of tests of a simulated model of a 45° swept-wing airplane in the Langley 9- by 12-inch supersonic blowdown tunnel indicate an effective upwash in the Mach number range from about 1.2 to 1.96. An effective upwash is shown in reference 1 at $M = 1.41$ for a design which is somewhat similar to the 45° swept-wing airplane of the present investigation. This effective upwash increases the static longitudinal stability and, hence, the control requirements for trim with an attendant drag increase.

Effect of nose length and body bump for model with aspect ratio of 3.7 and undrooped inlet.- The addition of the extended nose had a negligible effect on the lift, drag, and longitudinal stability (fig. 7) but resulted in what may be a serious reduction in directional stability $C_{n\beta}$ (fig. 8). Although a stable slope of $C_{n\beta}$ is obtained, it should

be pointed out that the sideslip results are for $\alpha = 0^\circ$ (slightly negative lift) and that the directional stability might be expected to decrease with increasing angle of attack.

The addition of the bump to the fuselage afterbody apparently results in a slight decrease in the minimum drag coefficient although the difference is within the accuracy of the drag measurements (fig. 7). The addition of the bump to the afterbody caused a slight increase in the lift at a given angle of attack and a reduction in the trim lift coefficient (fig. 7) for $i_t = -3^\circ$.

The directional stability for the bump-on configuration is slightly lower than that for the bump-off configuration (fig. 8). Although the directional stability for the basic-nose configuration, both with and without the bump, is considerably higher than the stability for the long-nose configuration, it should be remembered that the decrease in $C_{n\beta}$ expected with increasing angle of attack may still constitute a directional-stability problem.

The contribution of the tail to the sideslip derivatives at $\alpha = 0^\circ$ for the configuration having the basic nose, bump off, undrooped inlet, and $A = 3.7$ may be determined from the tail-on and tail-off results presented in figure 9. Although the lateral results for the complete model at $\alpha = 0^\circ$ (slight negative lift) indicate positive directional stability and slightly positive dihedral effect $-C_{l\beta}$, a complete evaluation of the lateral characteristics would require the determination of the effects of angle of attack on the sideslip derivatives as well as the effects of deflections of the directional and lateral control devices.

Effect of inlet droop on the configuration with basic nose, bump off, $A = 3.7$, and $i_t = -3^\circ$.— Although the difference is small, the droop of the forward part of the inlet from 0° to -5° apparently resulted in a slight increase in the minimum drag and a reduction in the rate of an increase in drag with increasing lift (fig. 10). The introduction of the droop also resulted in an increase in the angle of attack for zero lift and a reduction in the trim lift coefficient of about 0.025. These effects are similar to those that would be anticipated from the use of a cambered wing section.

Effect of aspect ratio on the configuration with basic nose, bump off, drooped inlet, and $i_t = -3^\circ$.— The results presented heretofore have been for the modified wing configuration (aspect ratio 3.7). A comparison of the modified wing configuration with the results for the basic wing configuration (aspect ratio 3.2) (fig. 11) indicates approximately a 10-percent increase in lift and a corresponding increase in longitudinal stability for the wing of higher aspect ratio. There was a slight but

measurable increase in minimum drag and maximum lift-drag ratio. (It should be pointed out that all coefficients throughout the report are based upon the geometry of the basic wing with aspect ratio 3.2.

Since the configuration with the lower aspect ratio had less longitudinal stability, it might be expected that the control requirements for trim would be less and the maximum trim lifts attainable might be greater than for the configuration with the higher aspect ratio. A comparison of the pitching-moment results (fig. 12(b) for $A = 3.2$ and fig. 4(b) for $A = 3.7$) indicates that this relationship does exist in that, although the tail effectiveness $\partial C_m / \partial i_t$ for a constant angle of attack is essentially the same for both aspect ratios, the increment in trim lift at $C_m = 0$ between $i_t = -3^\circ$ and $i_t = -8^\circ$ is greater for the lower aspect ratio configuration because of its lower stability. The actual values of trim lift obtained for the lower aspect ratio configuration at $i_t = -3^\circ$ and -8° (fig. 12) are less than those obtained for the higher aspect ratio configuration (fig. 4), but this difference is a result of the drooped inlet present for the model with $A = 3.2$ that was not present for the model with $A = 3.7$.

Effect of canopy shape and of inlet-wing transition fairing for configuration with basic nose, bump off, drooped inlet, and $A = 3.2$. Changing the vee-front canopy to a canopy having a small flat front had little effect on the minimum drag or on the aerodynamic characteristics in pitch for the complete model with $i_t = -8^\circ$ (fig. 12). A similar effect was found for the transition fairings between the inlet and the leading edge of the wing (fig. 13).

CONCLUSIONS

An investigation of the aerodynamic characteristics of several configurations of a model of a 45° swept-wing airplane at a Mach number of 2.01 in the Langley 4- by 4-foot supersonic pressure tunnel indicated the following conclusions:

1. Configurations employing the wing of increased aspect ratio ($A = 3.7$), which constituted the bulk of the tests, produced about a 10-percent increase in lift and in longitudinal stability compared to that for the basic wing of aspect ratio 3.2. There was a slight but measurable increase in minimum drag and maximum lift-drag ratio.
2. For the basic configuration modified to the wing of aspect ratio 3.7, the maximum horizontal tail deflection of -16° resulted in a trim lift coefficient of about 0.3 at an angle of attack of 7.7° , a trim drag coefficient of 0.086, and a trim lift-drag ratio of 3.5. The minimum trim drag coefficient for a horizontal tail deflection of -3° was about 0.035.

3. An effective upwash at the low horizontal tail contributed to the high degree of longitudinal stability.

4. At zero angle of attack (slight negative lift), the basic configuration with the modified wing of $A = 3.7$ indicated positive directional and lateral stability.

5. The addition of the extended nose to the body had a negligible effect on the lift, drag, and longitudinal stability but reduced the directional stability to such an extent that instability might occur with increasing angle of attack.

6. The droop of the forward part of the inlet resulted in a slight increase in minimum drag, a decrease in the variation of drag with lift, and a reduction in the trim lift coefficient of about 0.025.

7. The addition of the bump to the fuselage afterbody apparently resulted in a slight reduction in minimum drag although the difference was within the accuracy of the drag measurements.

8. The use of a flat-front canopy instead of a vee-front canopy or the addition of various transition fairings between the inlet and leading edge of the wing had little effect on the drag or the aerodynamic characteristics in pitch.

Langley Aeronautical Laboratory,
National Advisory Committee for Aeronautics,
Langley Field, Va., September 21, 1954.

REFERENCE

1. Palazzo, Edward B., and Spearman, M. Leroy: Static Longitudinal and Lateral Stability and Control Characteristics of a Model of a 35° Swept-Wing Airplane at a Mach Number of 1.41. NACA RM L54G08, 1955.

TABLE I

GEOMETRIC CHARACTERISTICS OF A MODEL OF A 45° SWEEP-WING AIRPLANE

Wing:

Aspect ratio, basic wing	3.2
Aspect ratio with extended tips	3.7
Span, basic wing, ft	1.591
Span with extended tips, ft	1.77
Area, basic wing (excluding inlets), sq ft	0.795
Area with extended tips, sq ft	0.848
Taper ratio, basic wing	0.468
Taper ratio with extended tips	0.406
Sweep at quarter-chord line, deg	45
Dihedral measured in chord plane, deg	-3.5
Twist, deg	0
Incidence, deg	0
Section, inboard (0.38b/2 station)	NACA 65A005.5
Section, tip	NACA 65A003.7
Mean aerodynamic chord, basic wing, ft	0.522
Mean aerodynamic chord with extended tips, ft	0.507

Fuselage:

Length, basic, ft	2.736
Length, extended nose, ft	3.05
Width, maximum, ft	0.199
Depth, maximum (excluding canopy), ft	0.296
Frontal area, sq ft	0.051

Horizontal tail:

Area, including body intercept, sq ft	0.188
Span, ft	0.758
Aspect ratio	3.06
Taper ratio	0.456
Sweep at quarter-chord line, deg	45
Dihedral, deg	0
Twist, deg	0
Section, root	NACA 65A006
Section, tip	NACA 65A004
Mean aerodynamic chord, ft	0.26
Hinge line, percent tail mean aerodynamic chord	0.098
Tail length from $\frac{\bar{c}}{4}$ of wing to $\frac{\bar{c}}{4}$ of tail, ft	0.94

Vertical tail:

Area (to body center line), sq ft	0.155
Span (to body center line), ft	0.496
Aspect ratio	1.593
Taper ratio	0.365
Sweep at quarter-chord line, deg	45
Section, inboard	NACA 65A006
Section, tip	NACA 65A004
Mean aerodynamic chord, ft	0.334
Tail length from $\frac{\bar{c}}{4}$ of wing to $\frac{\bar{c}}{4}$ of vertical tail, ft	0.791

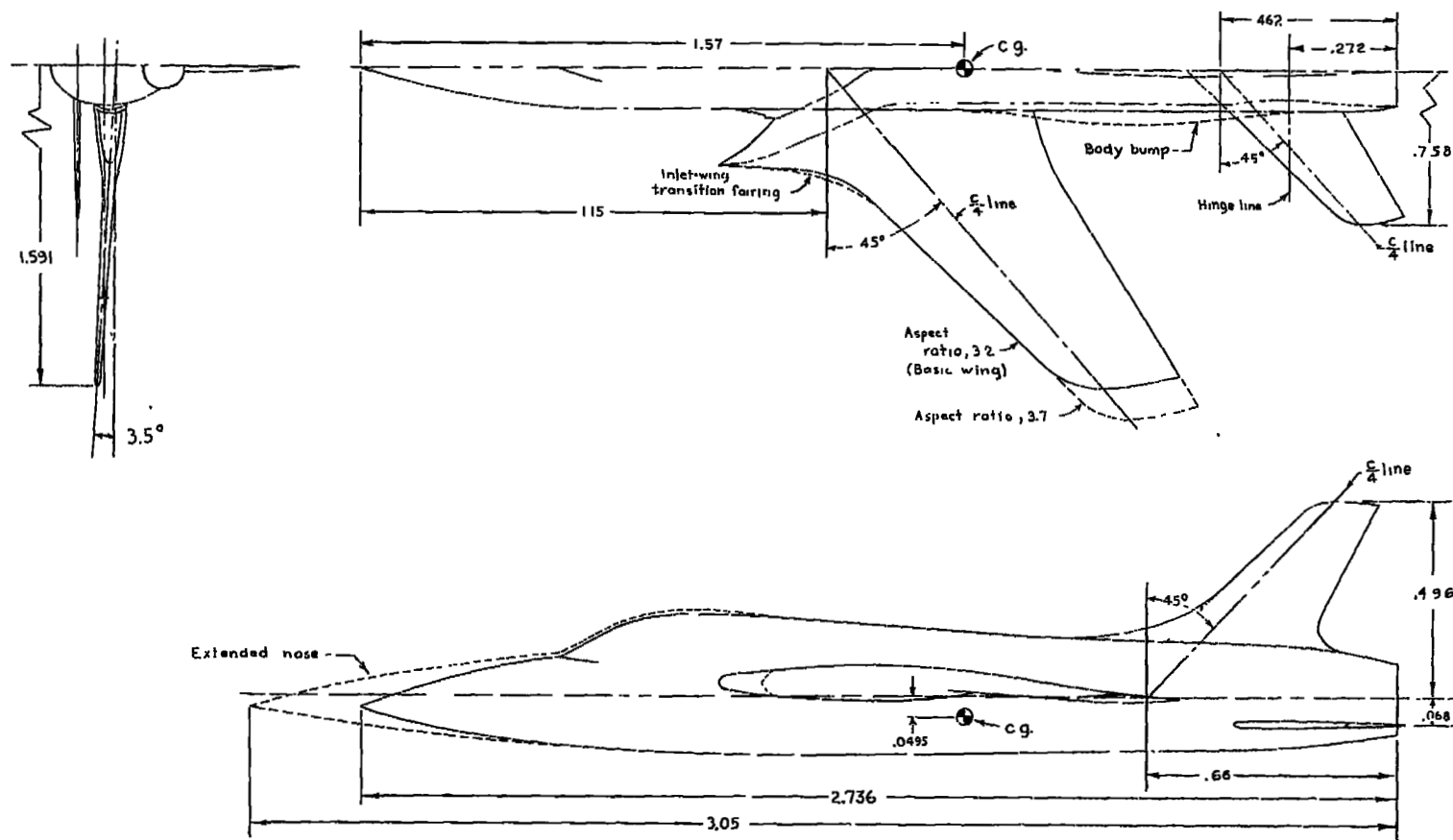


Figure 1.- Three-view drawing of model of a 45° swept-wing airplane. Solid lines define basic model. All dimensions are in feet unless otherwise noted.

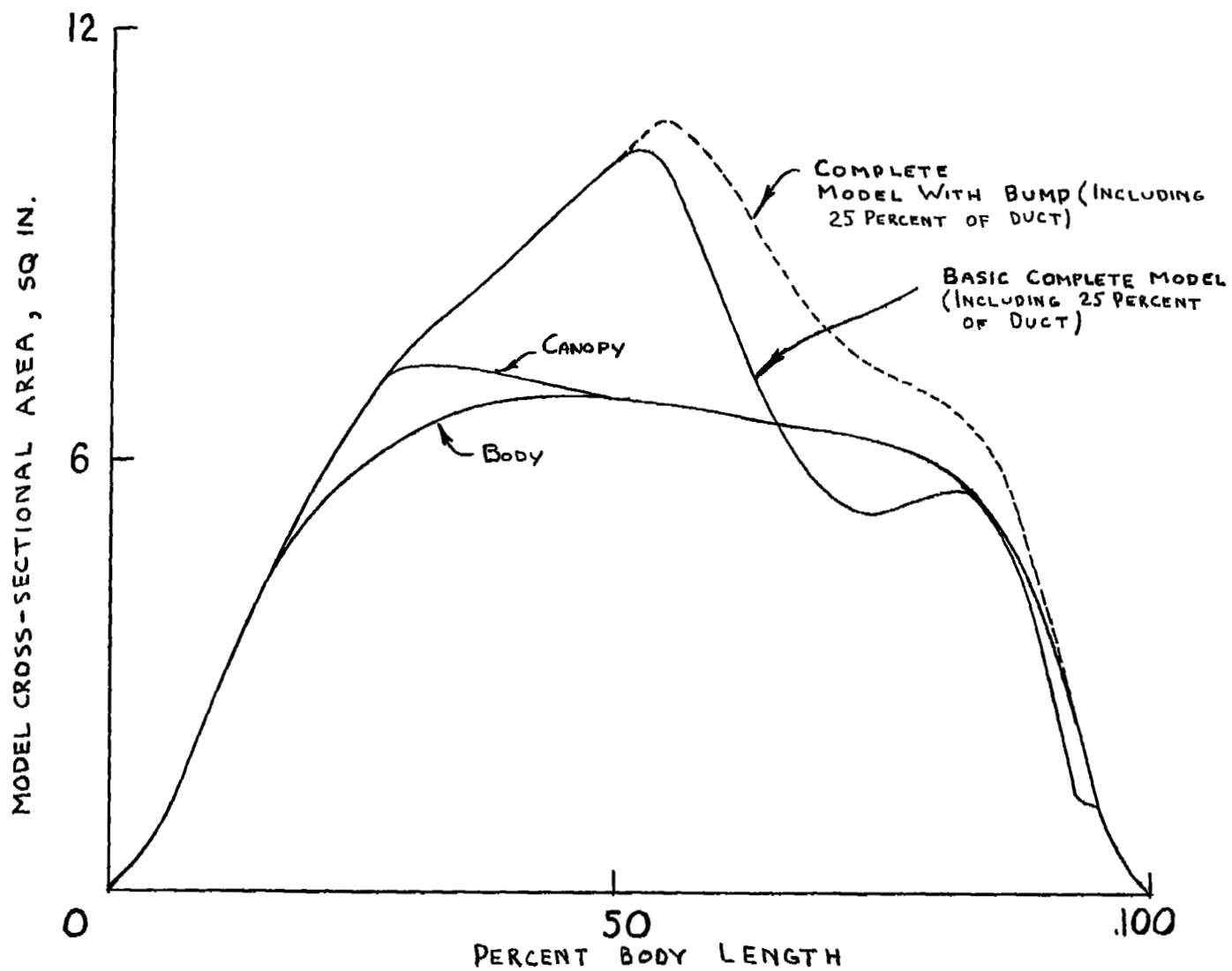
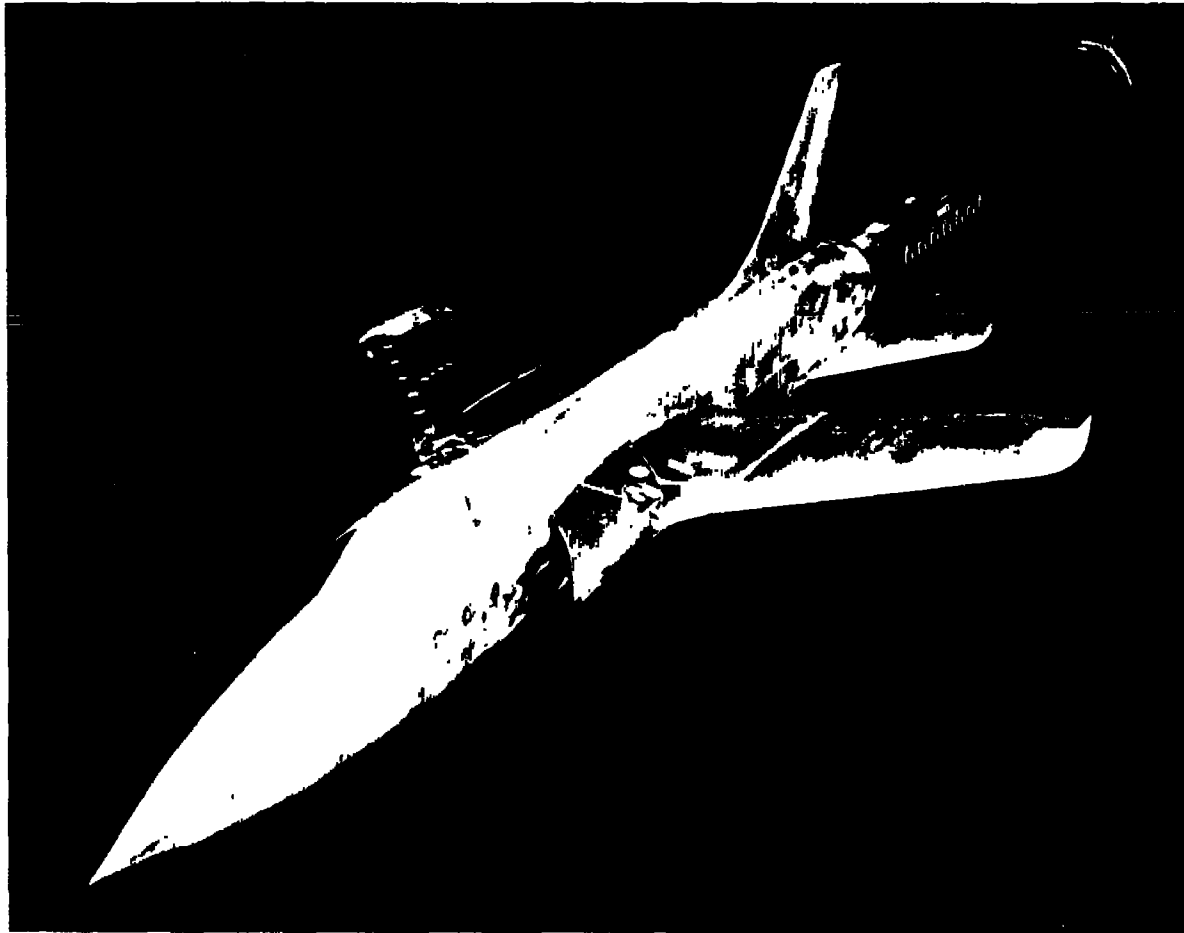


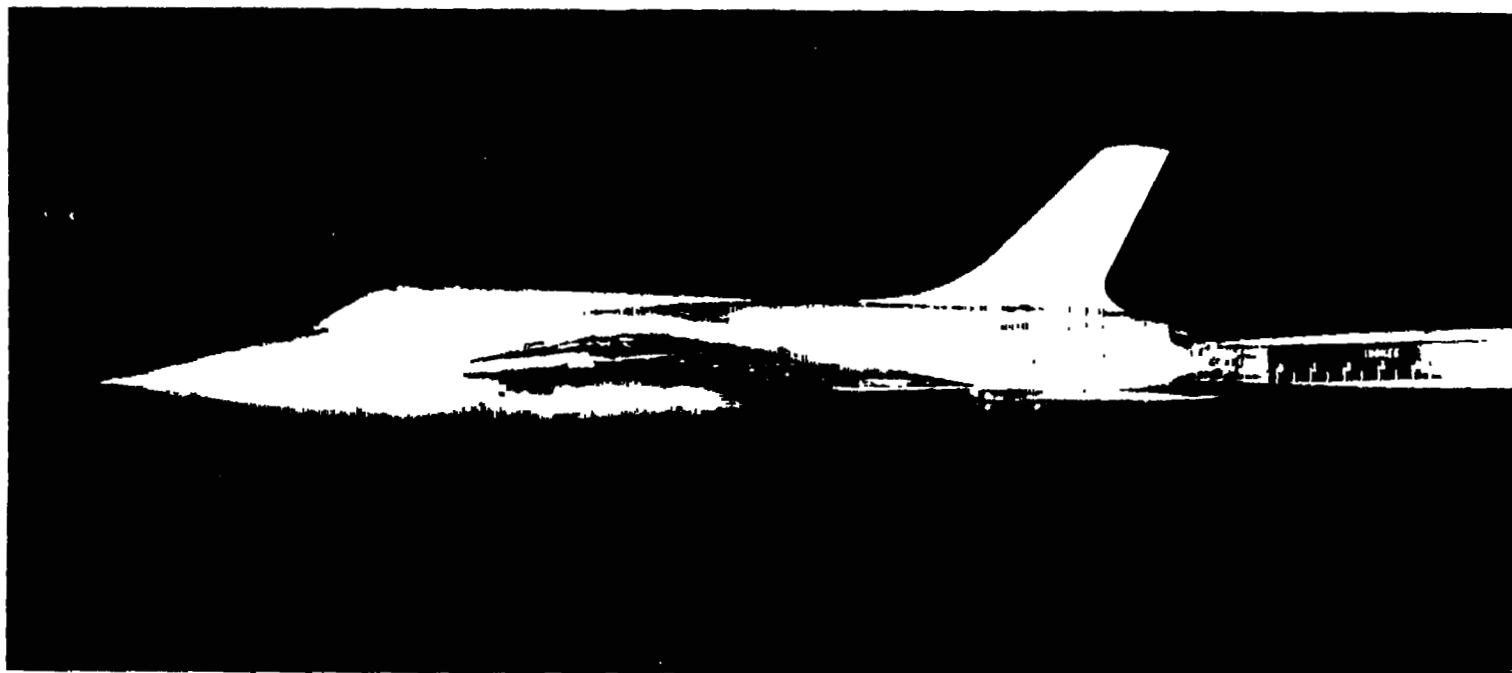
Figure 2.- Longitudinal area distribution of model.



(a) Right front view.

L-84802

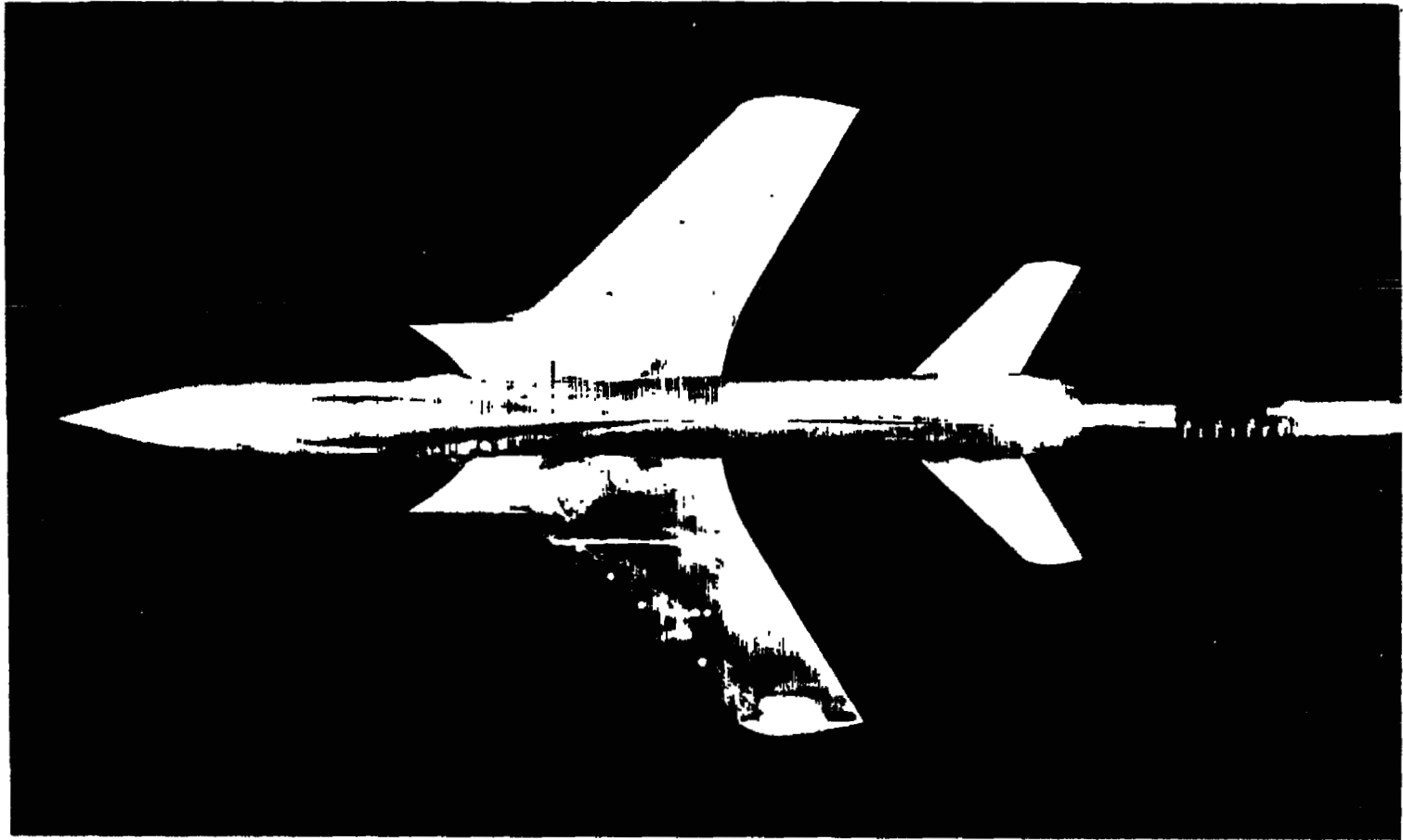
Figure 3.- Photographs of model with basic nose and wing, drooped inlets,
and bump off.



(b) Side view.

L-84801

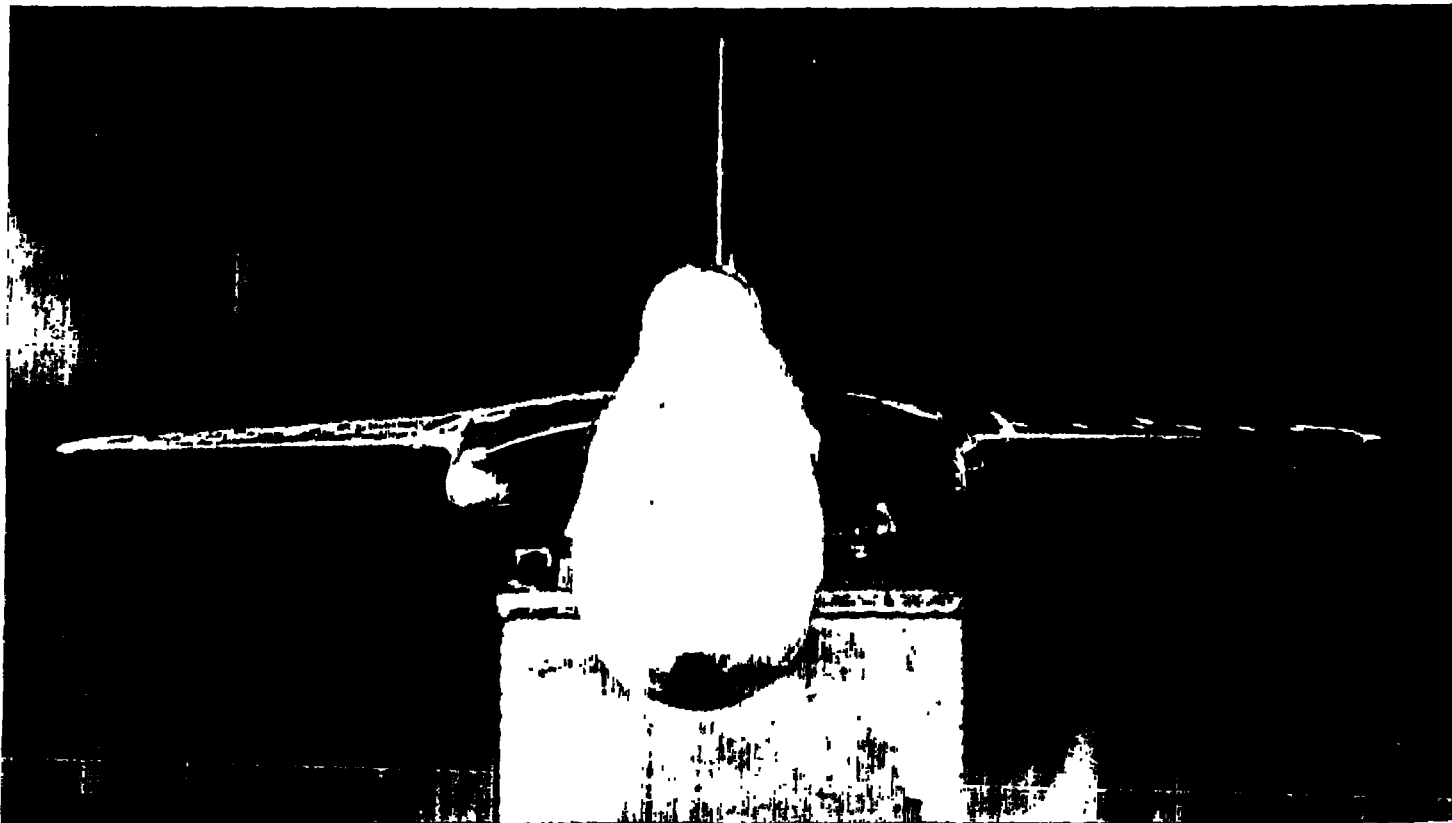
Figure 3.- Continued.



(c) Bottom view.

L-84800

Figure 3.- Continued.



(d) Front view.

L-84799

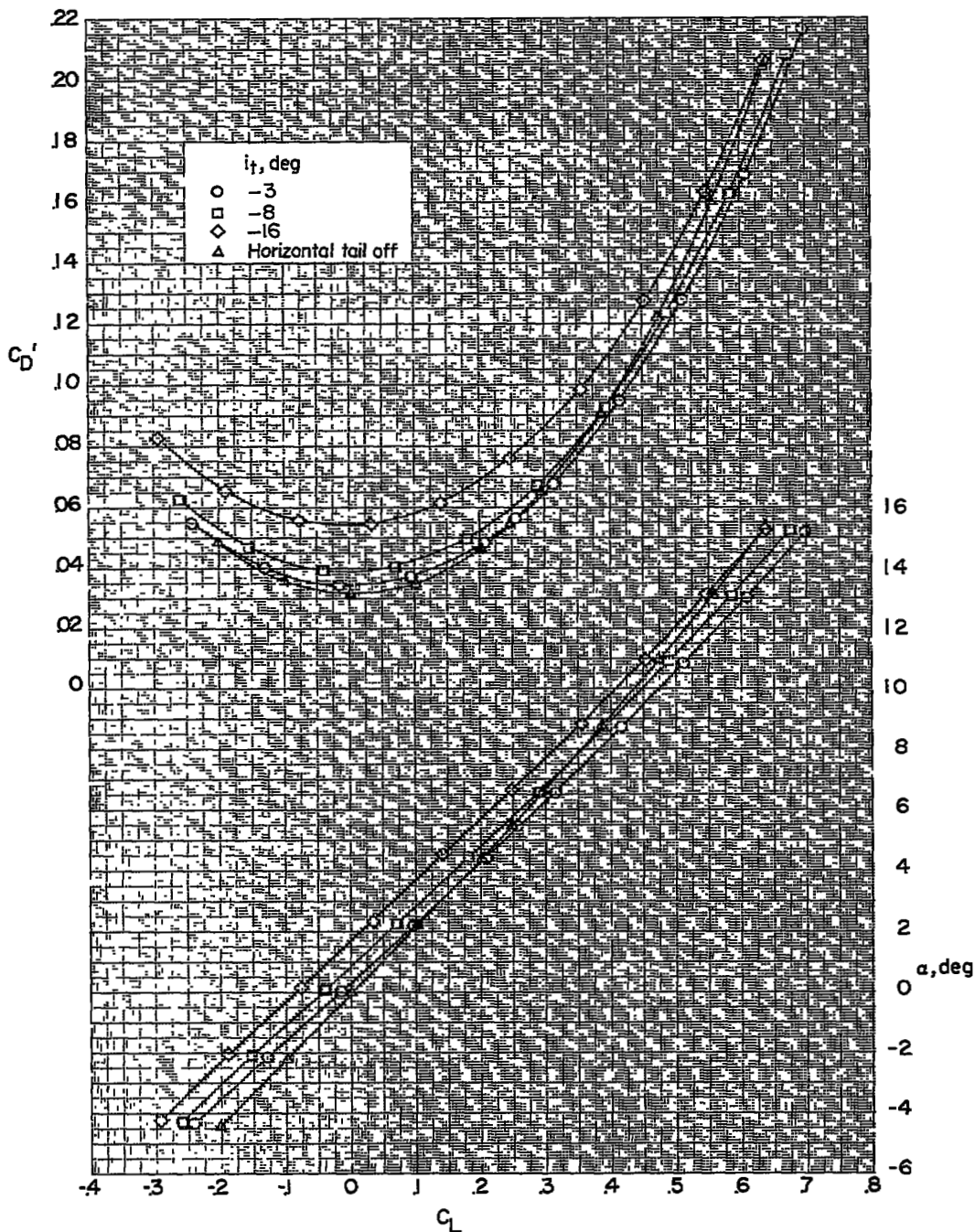
Figure 3.- Continued.



(e) Top view. 0° transition fairing.

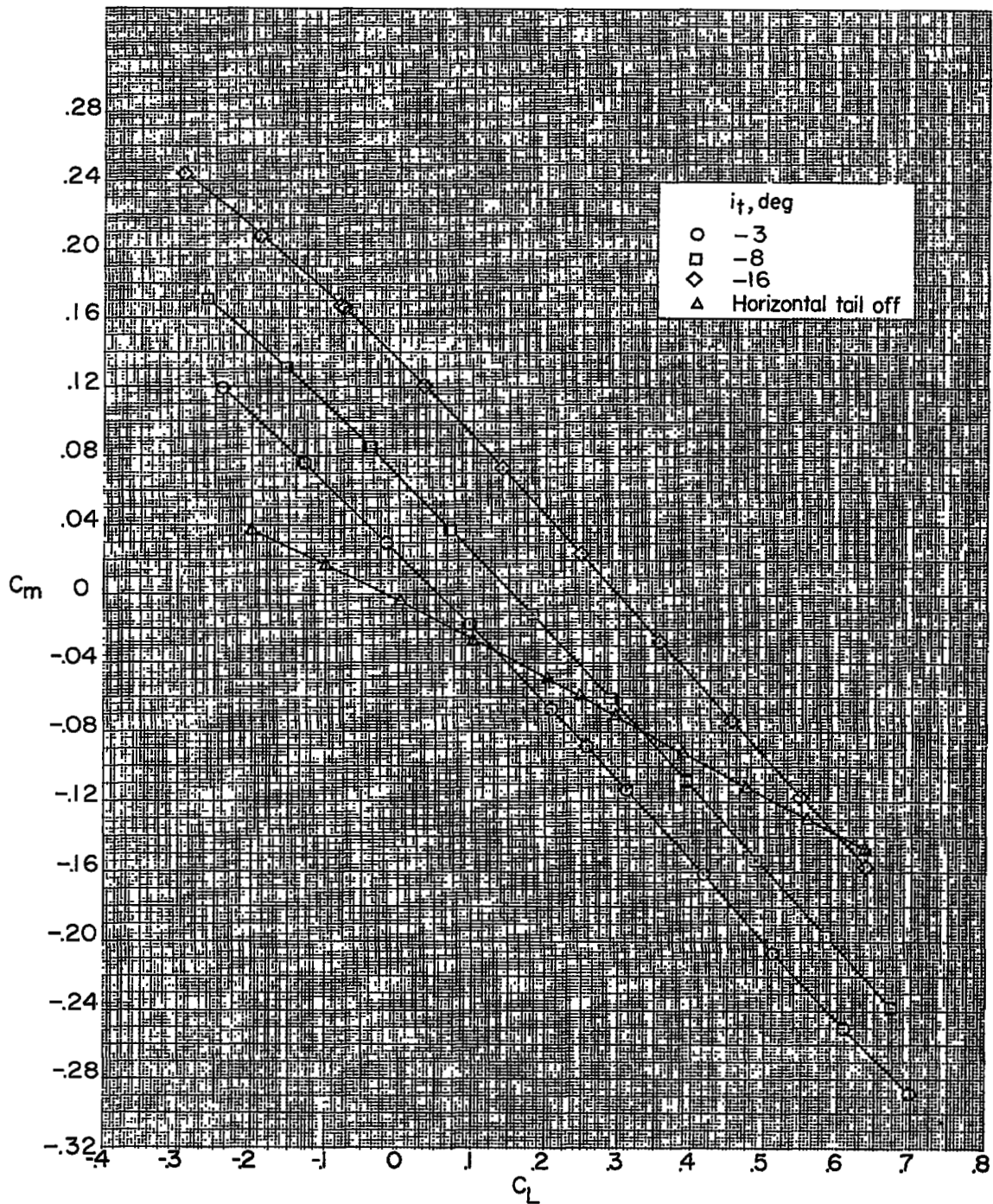
L-86422

Figure 3.- Concluded.



(a) Variation of drag coefficient and angle of attack with lift coefficient.

Figure 4.- Effect of horizontal tail on aerodynamic characteristics in pitch. Basic nose; bump off; $A = 3.7$; undrooped inlet.



(b) Variation of pitching-moment coefficient with lift coefficient.

Figure 4.- Concluded.

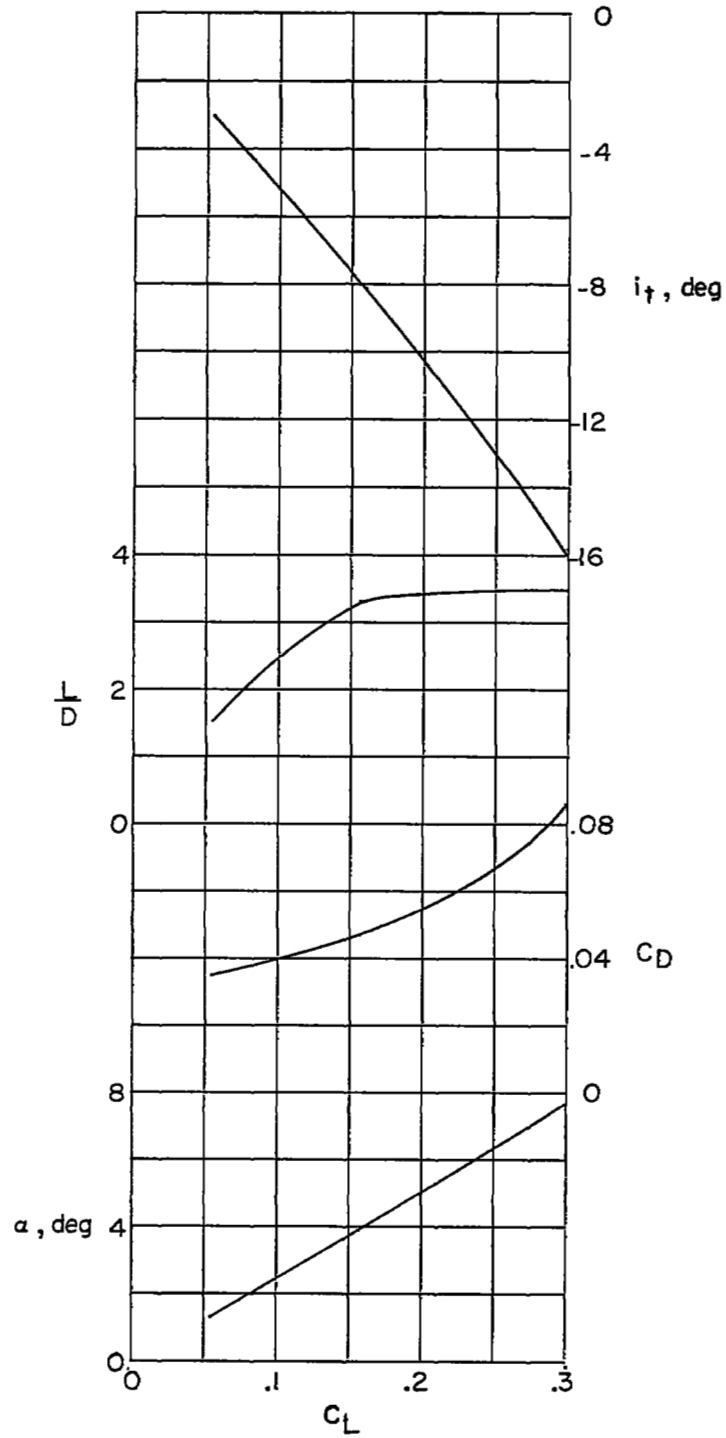
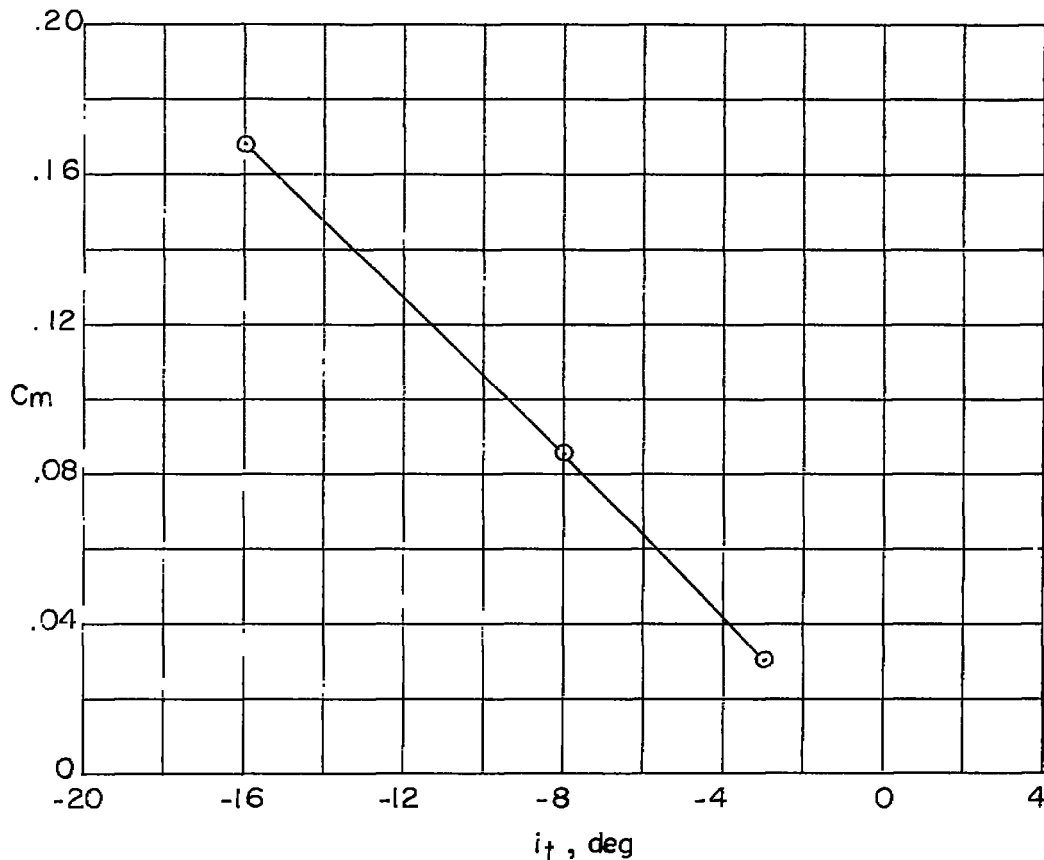
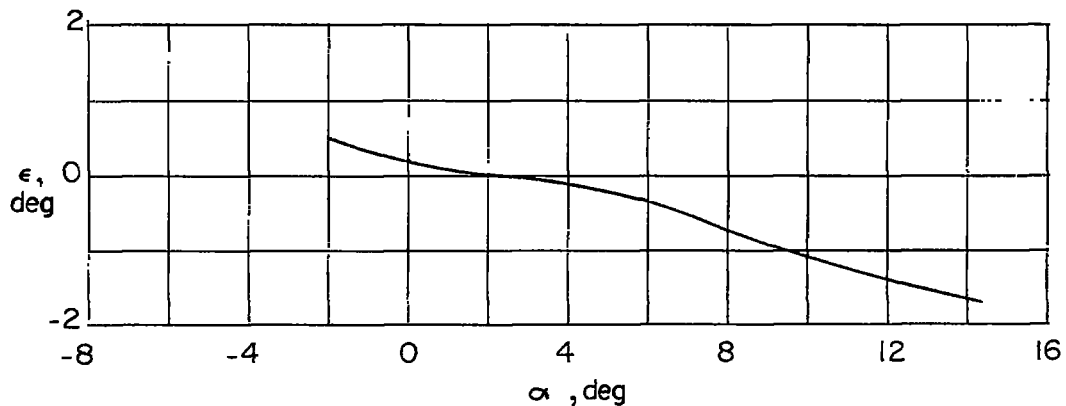


Figure 5.- Longitudinal characteristics for trim, $C_m = 0$. Basic nose; bump off; $A = 3.7$; undrooped inlet.

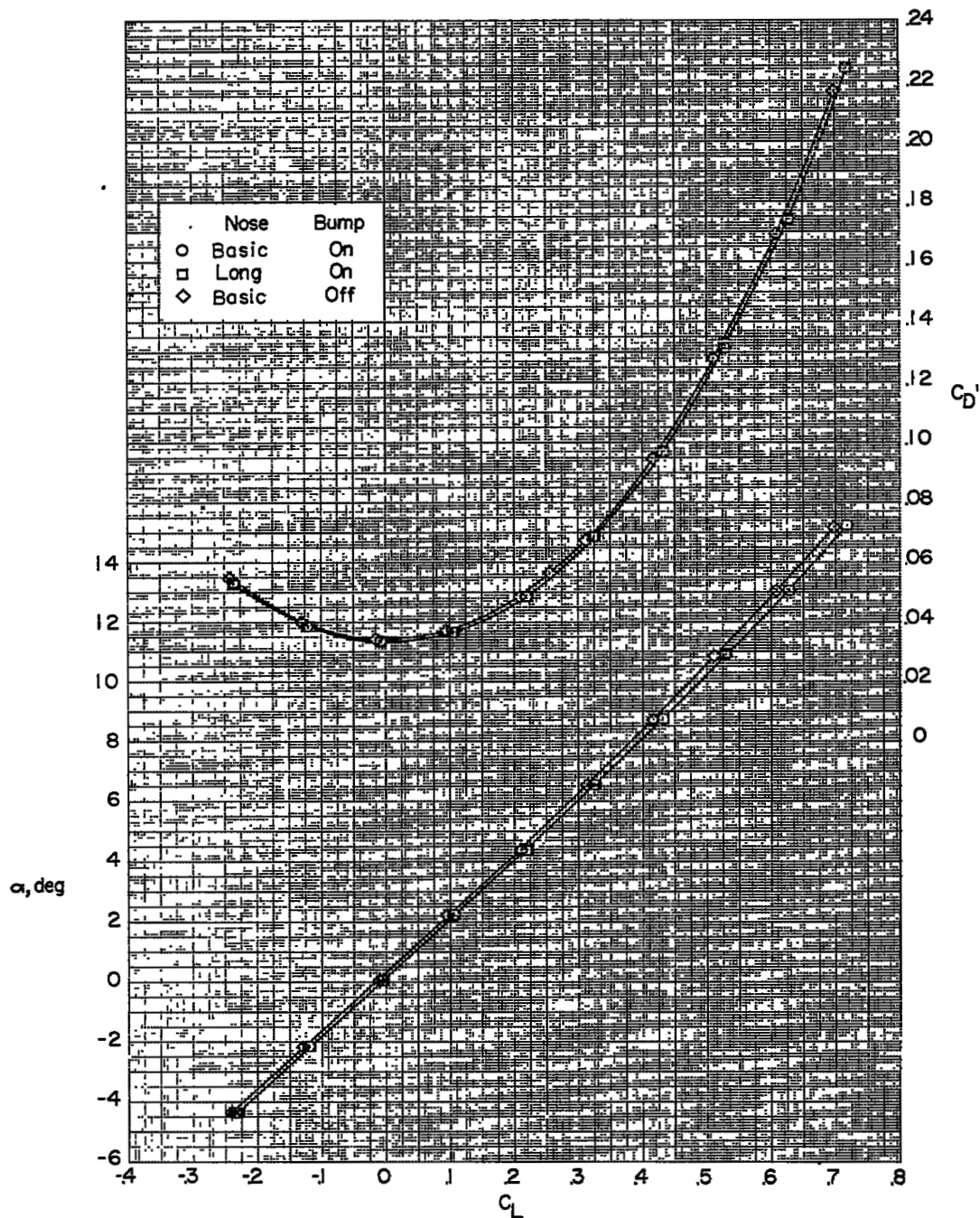


(a) Variation of pitching-moment coefficient with angle of incidence of horizontal tail.



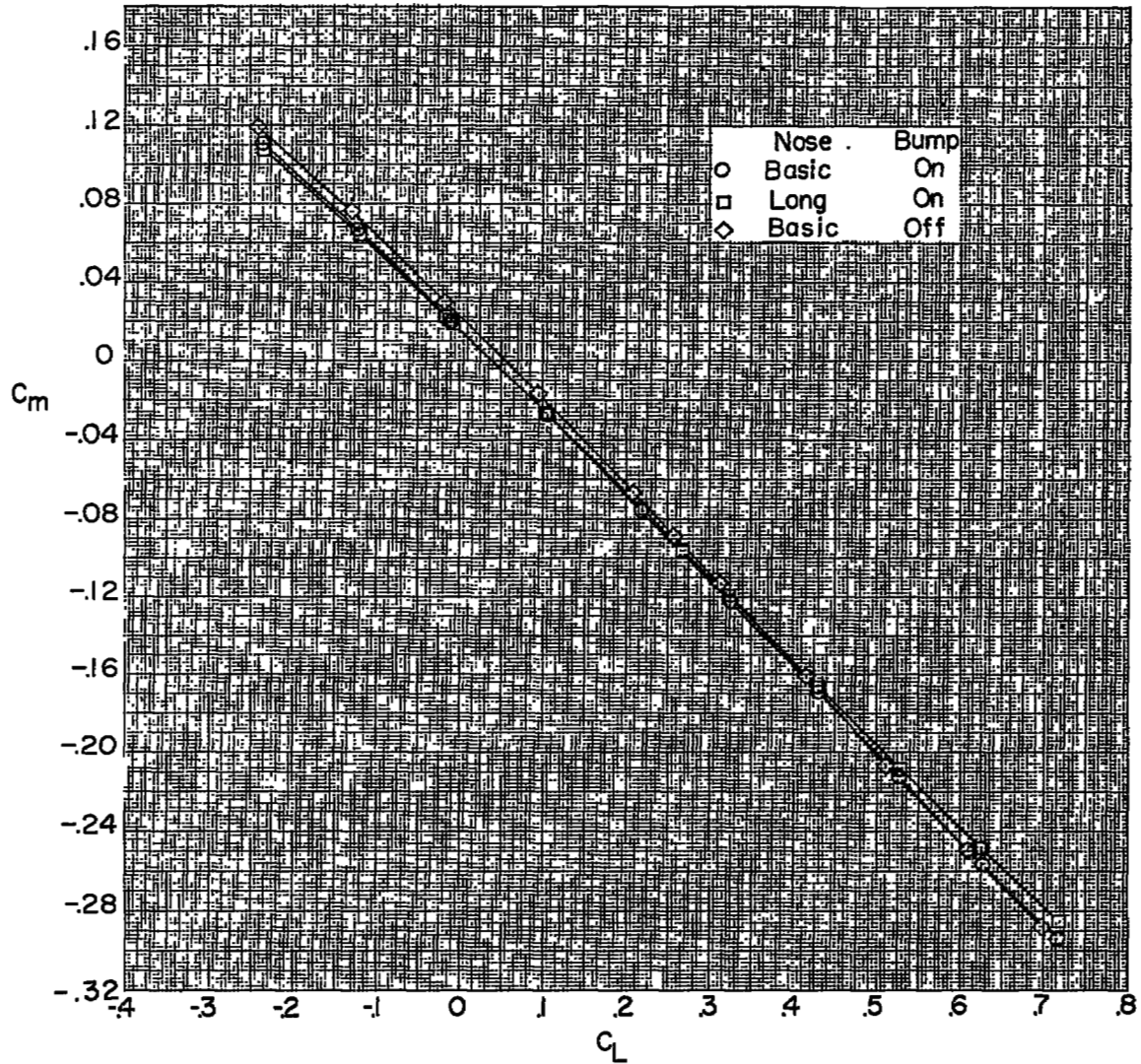
(b) Variation of effective downwash with angle of attack.

Figure 6.- Pitching effectiveness and downwash characteristics of tail.
Basic nose; bump off; $A = 3.7$; undrooped inlet.



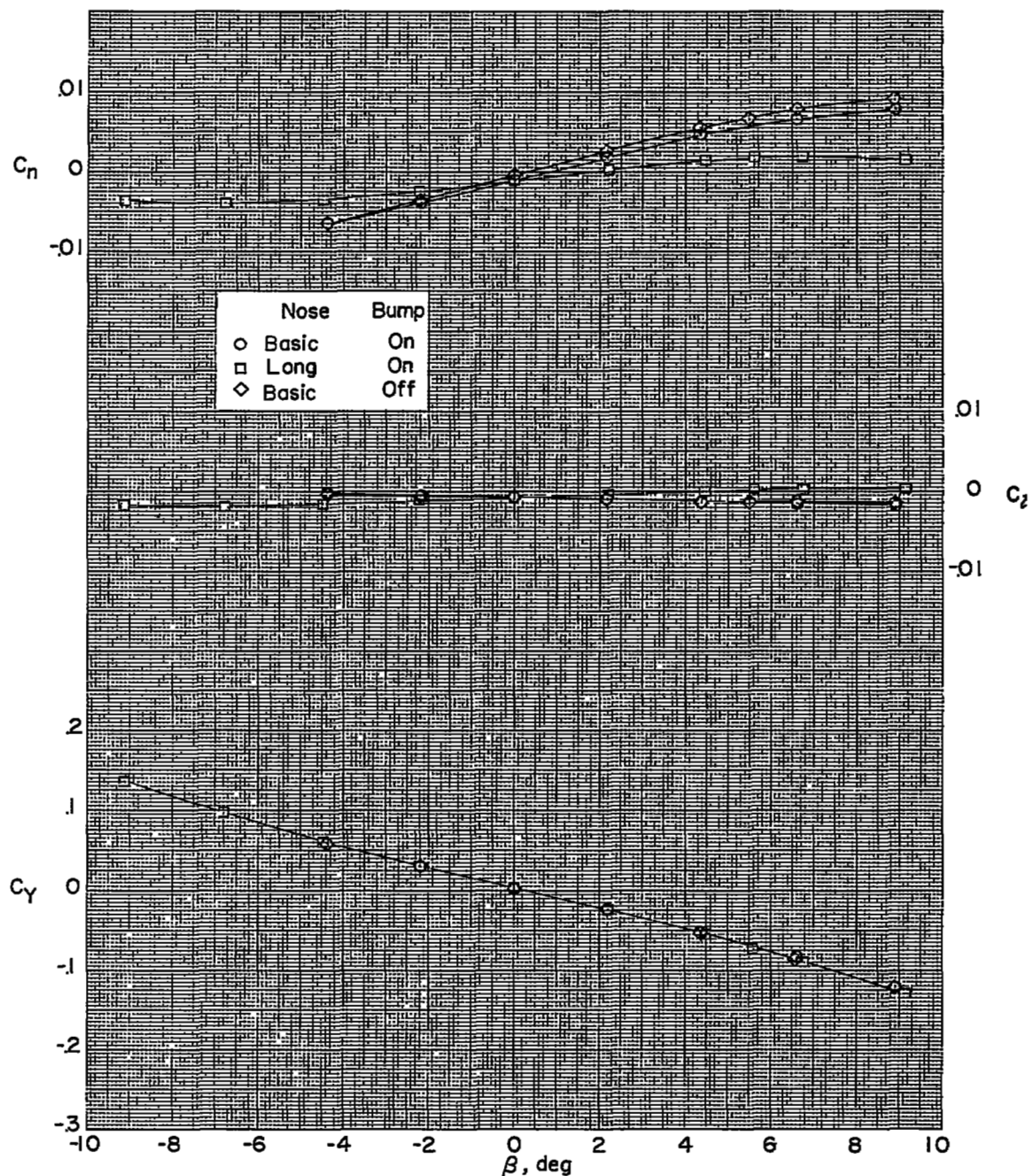
(a) Variation of drag coefficient and angle of attack with lift coefficient.

Figure 7.- Effect of nose length and body bump on aerodynamic characteristics in pitch. $A = 3.7$; undrooped inlet; $i_t = -3^\circ$.



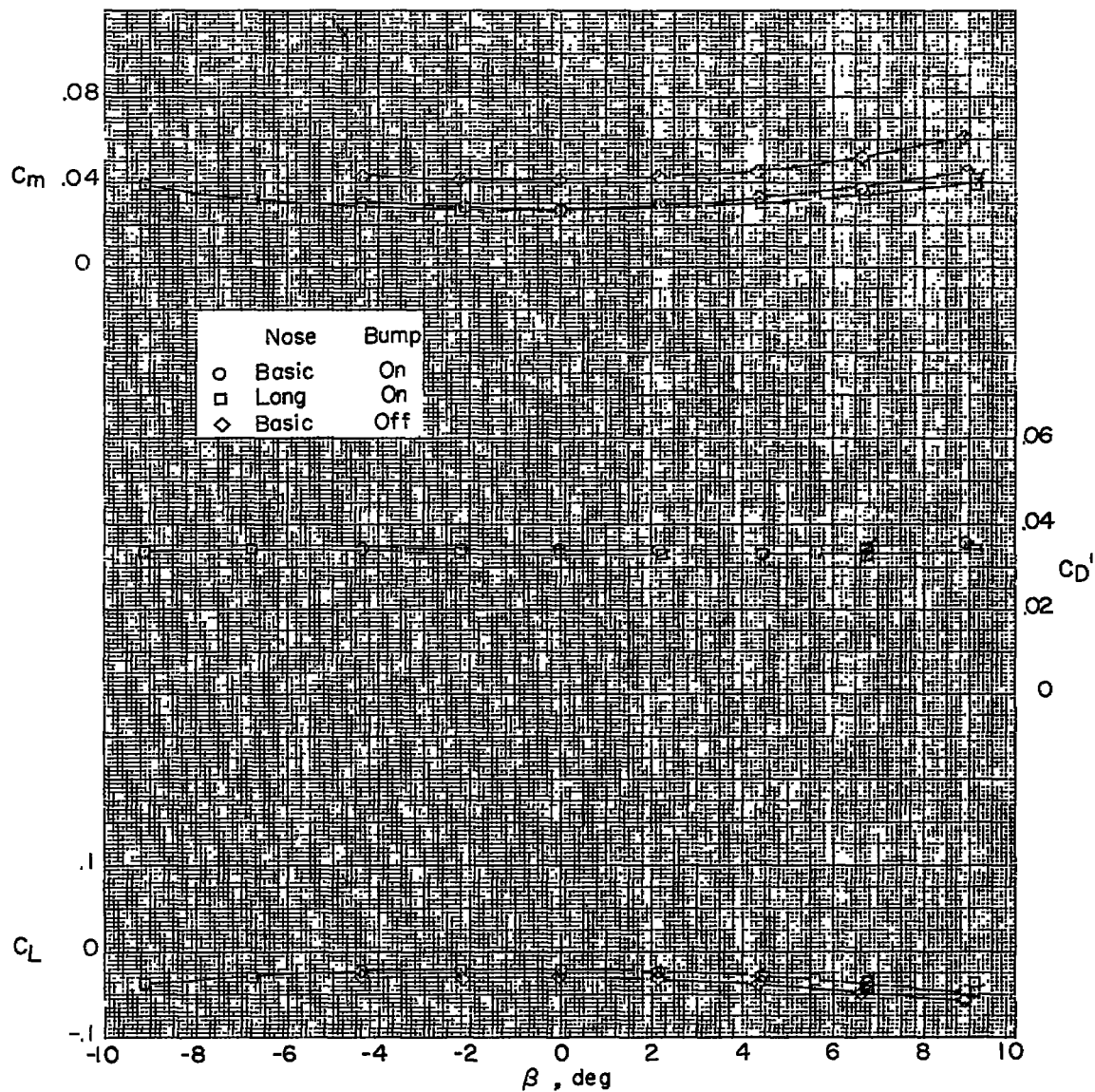
(b) Variation of pitching-moment coefficient with lift coefficient.

Figure 7.- Concluded.



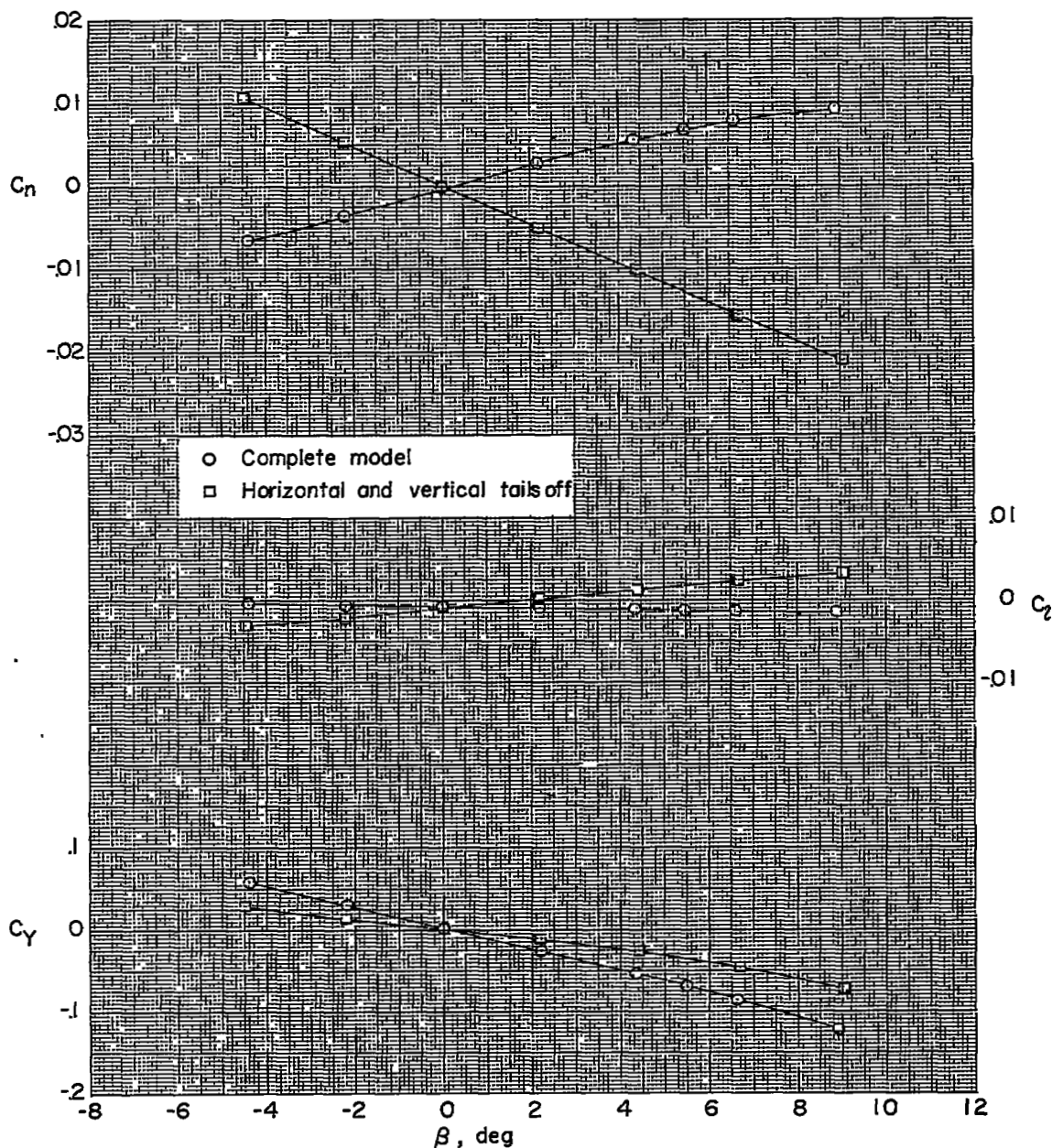
(a) Variation of yawing-moment coefficient, rolling-moment coefficient, and side-force coefficient with angle of sideslip.

Figure 8.- Effect of nose length and body bump on aerodynamic characteristics in sideslip. $A = 3.7$; undrooped inlet; $\alpha = 0^\circ$; $i_t = -3^\circ$.



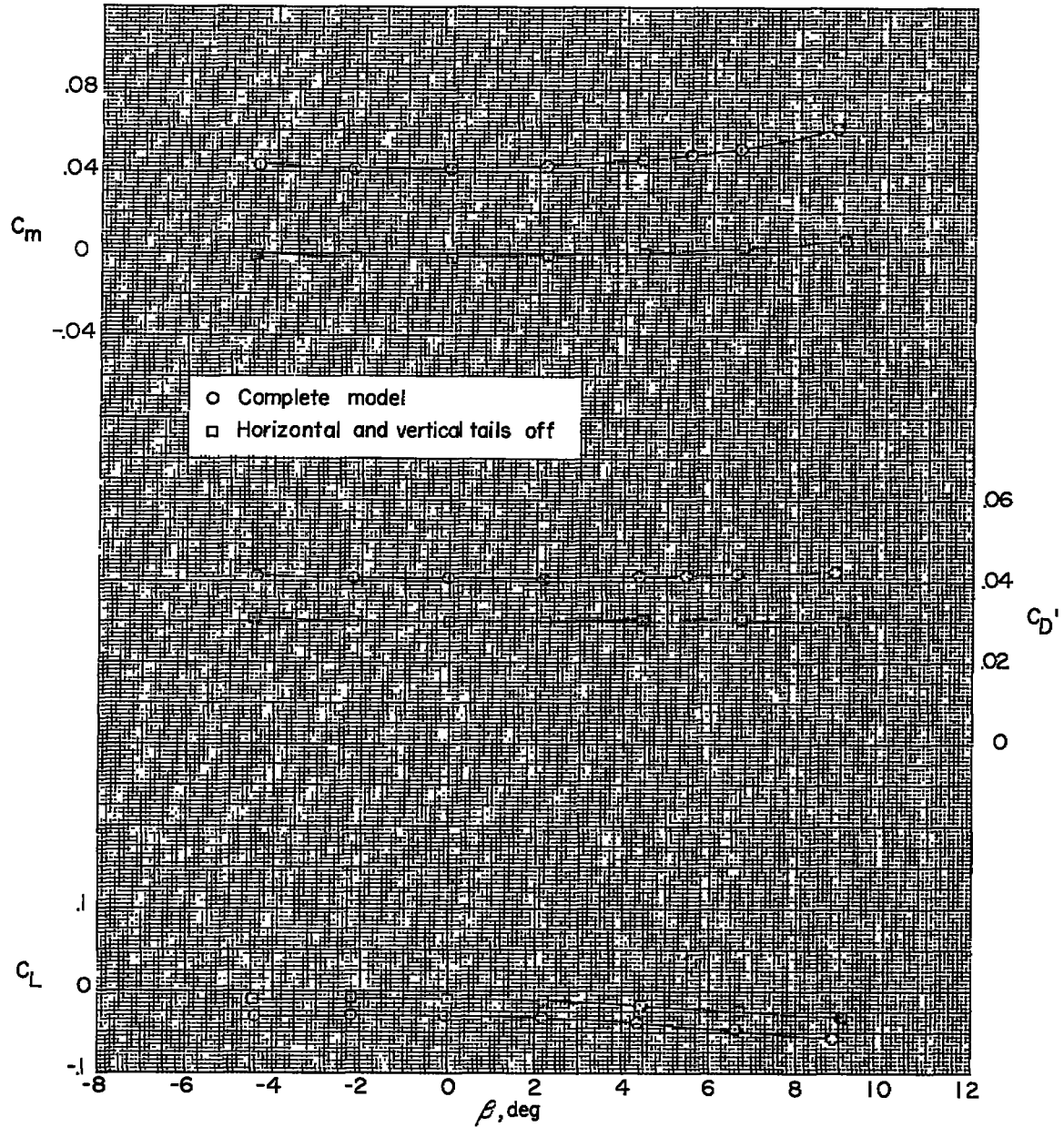
(b) Variation of pitching-moment coefficient, drag coefficient, and lift coefficient with angle of sideslip.

Figure 8.- Concluded.



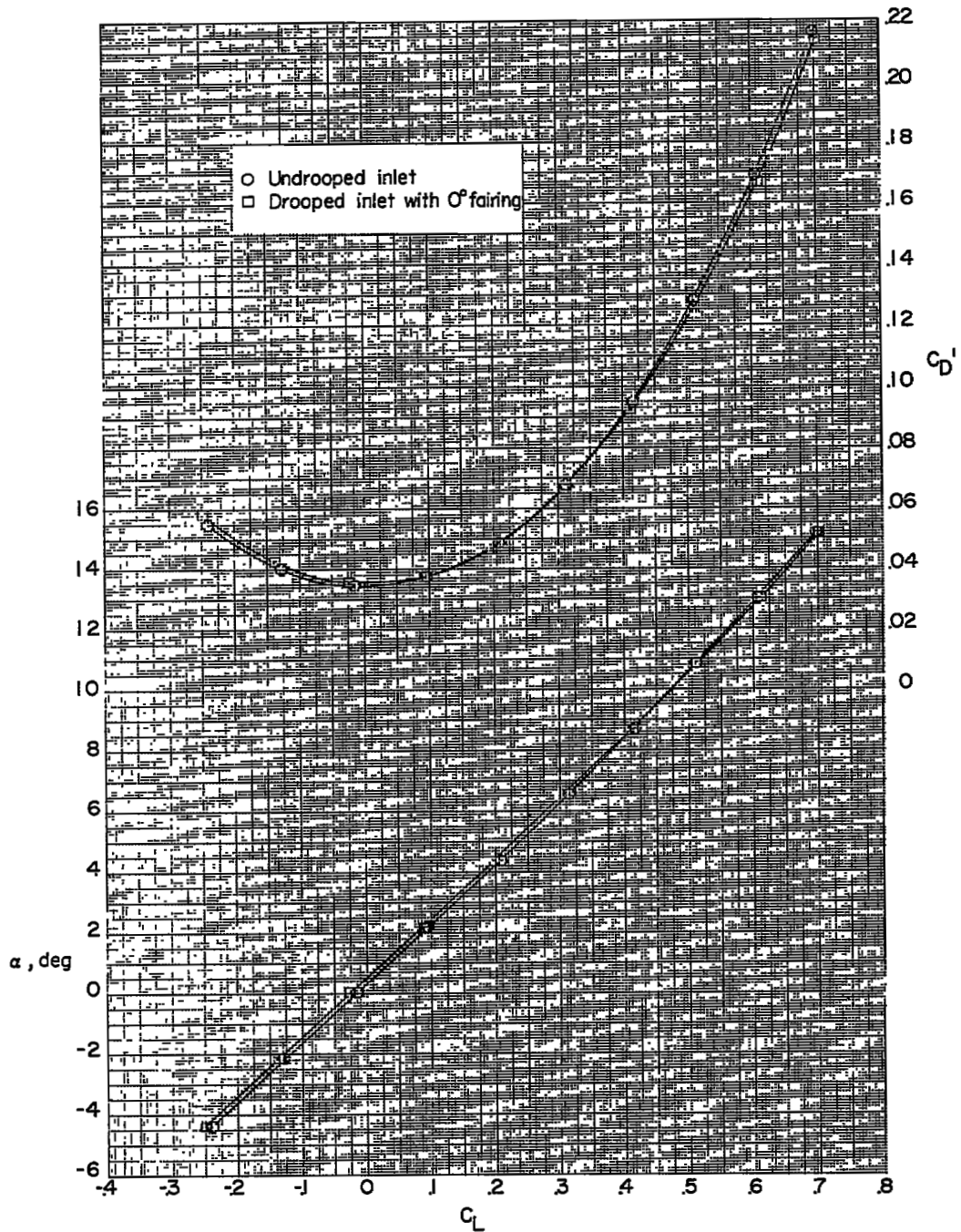
(a) Variation of yawing-moment coefficient, rolling-moment coefficient, and side-force coefficient with angle of sideslip.

Figure 9.- Aerodynamic characteristics in sideslip. Basic nose; bump off; undrooped inlet; $A = 3.7$; $\alpha = 0^\circ$.



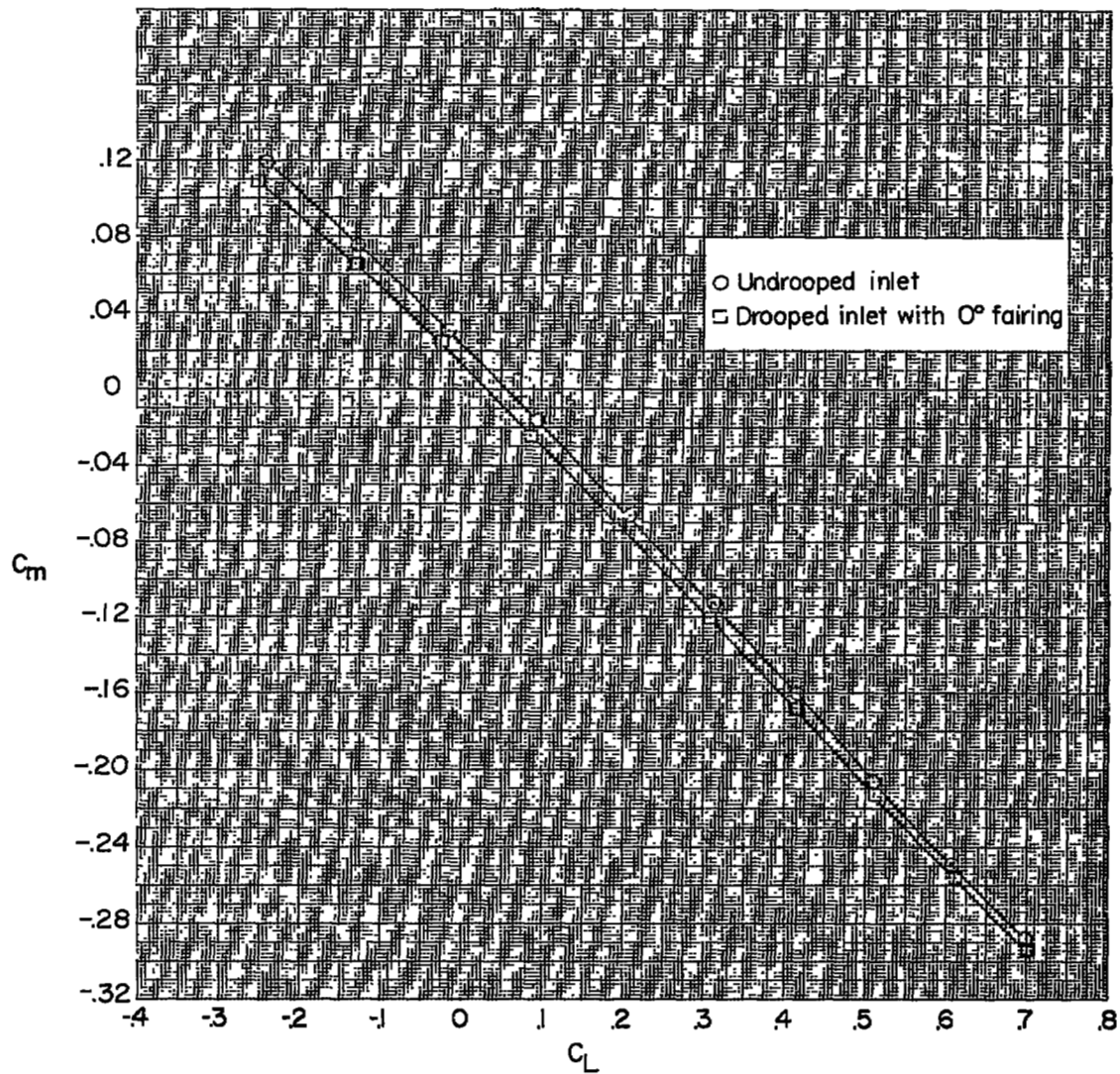
(b) Variation of pitching-moment coefficient, drag coefficient, and lift coefficient with angle of sideslip.

Figure 9.- Concluded.



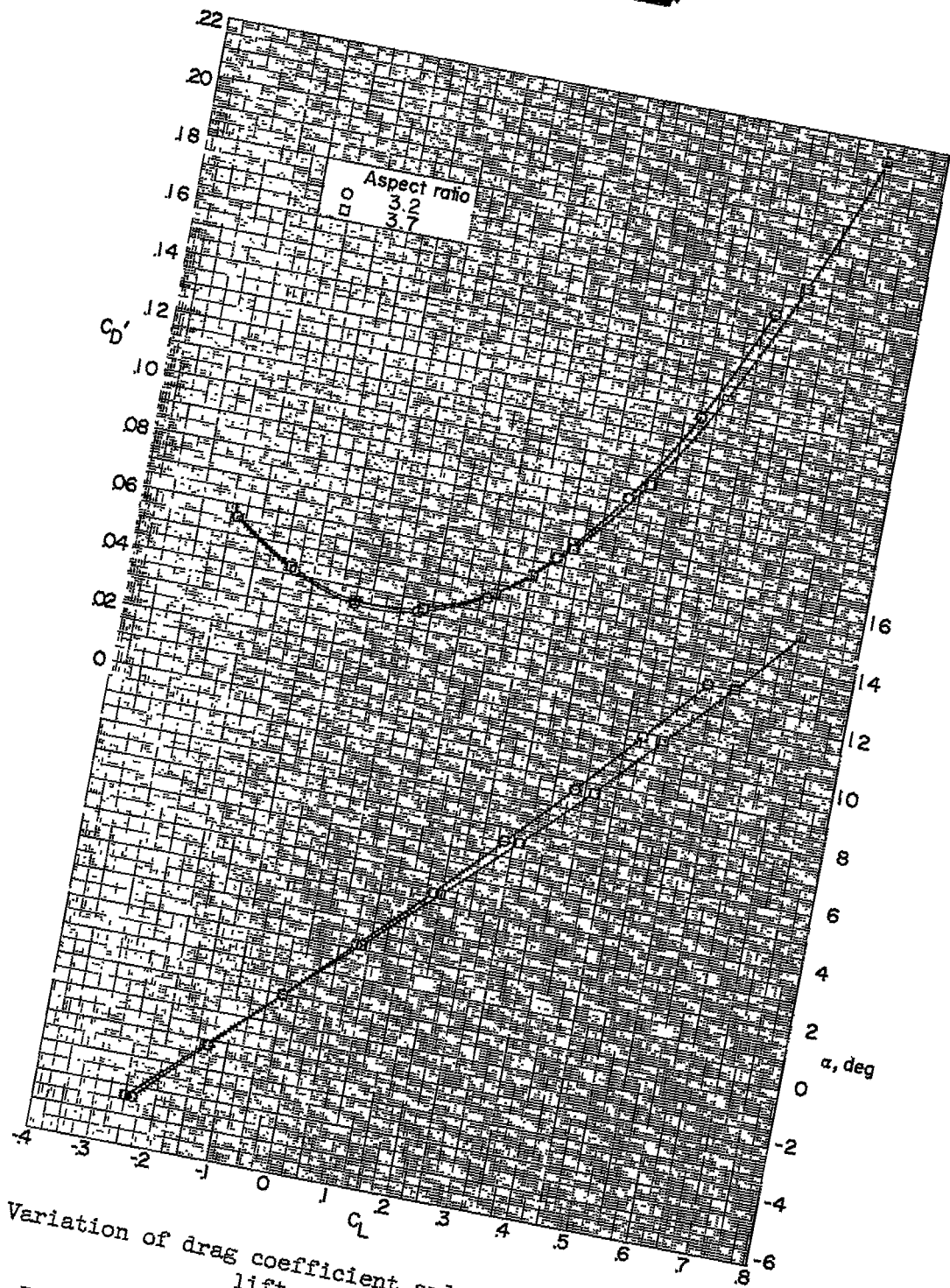
(a) Variation of drag coefficient and angle of attack with lift coefficient.

Figure 10.- Effect of inlet droop on aerodynamic characteristics in pitch. Basic nose; bump off; $A = 3.7$; $i_t = -3^\circ$.



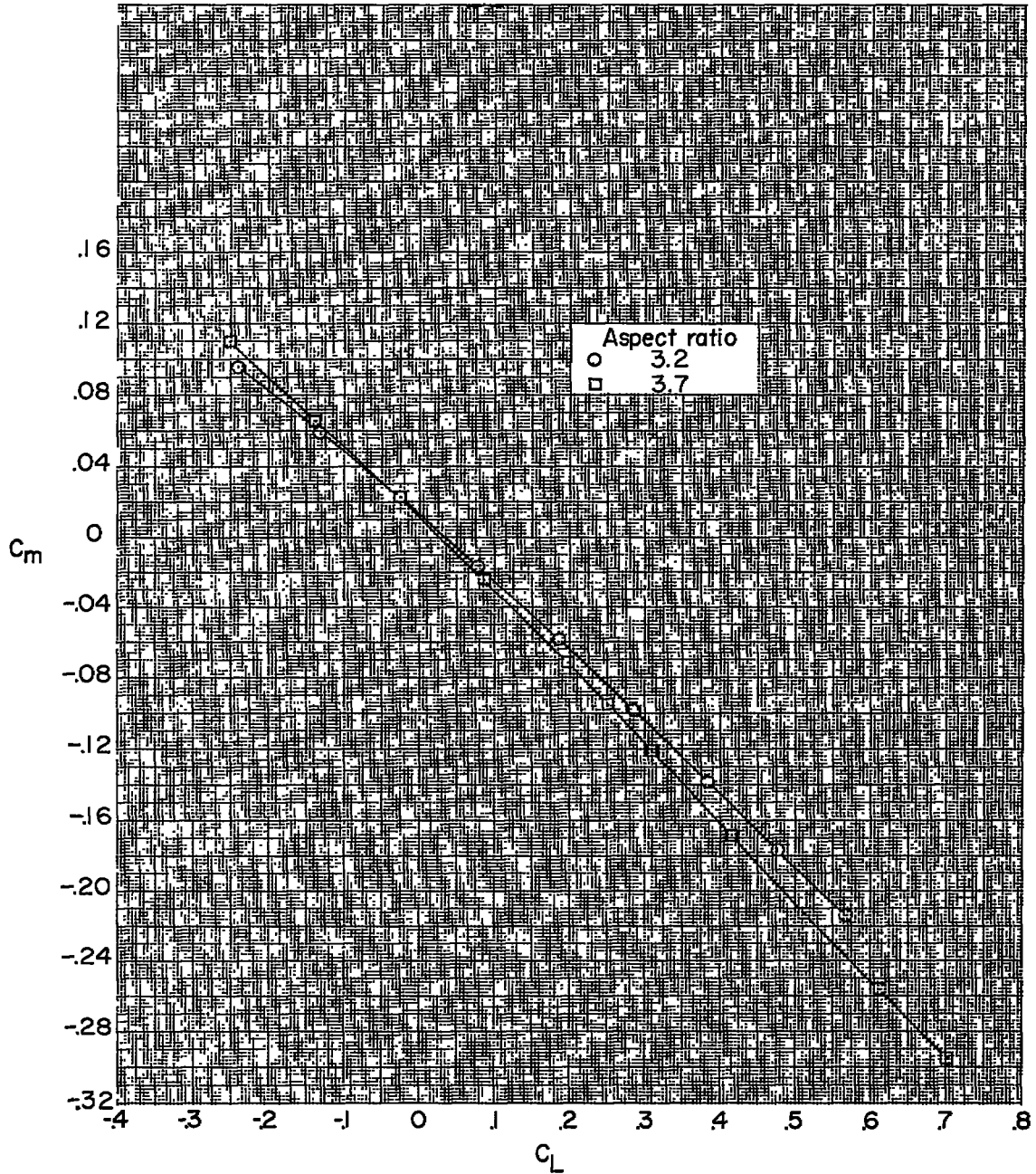
(b) Variation of pitching-moment coefficient with lift coefficient.

Figure 10.- Concluded.



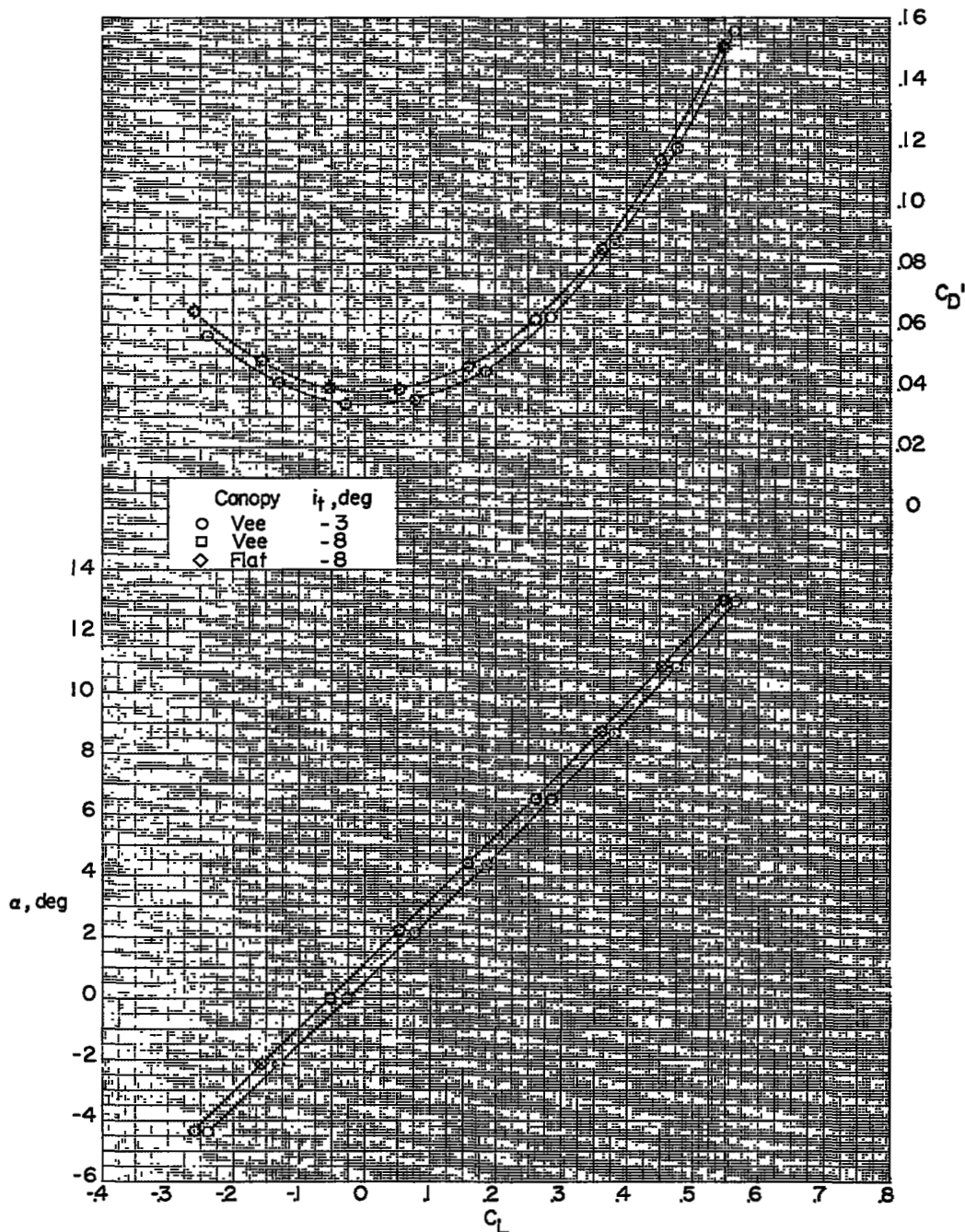
(a) Variation of drag coefficient and angle of attack with lift coefficient.

Figure 11.- Effect of aspect ratio on aerodynamic characteristics in pitch. Basic nose; bump off; drooped inlet with 0° fairing; $i_t = -3^\circ$.



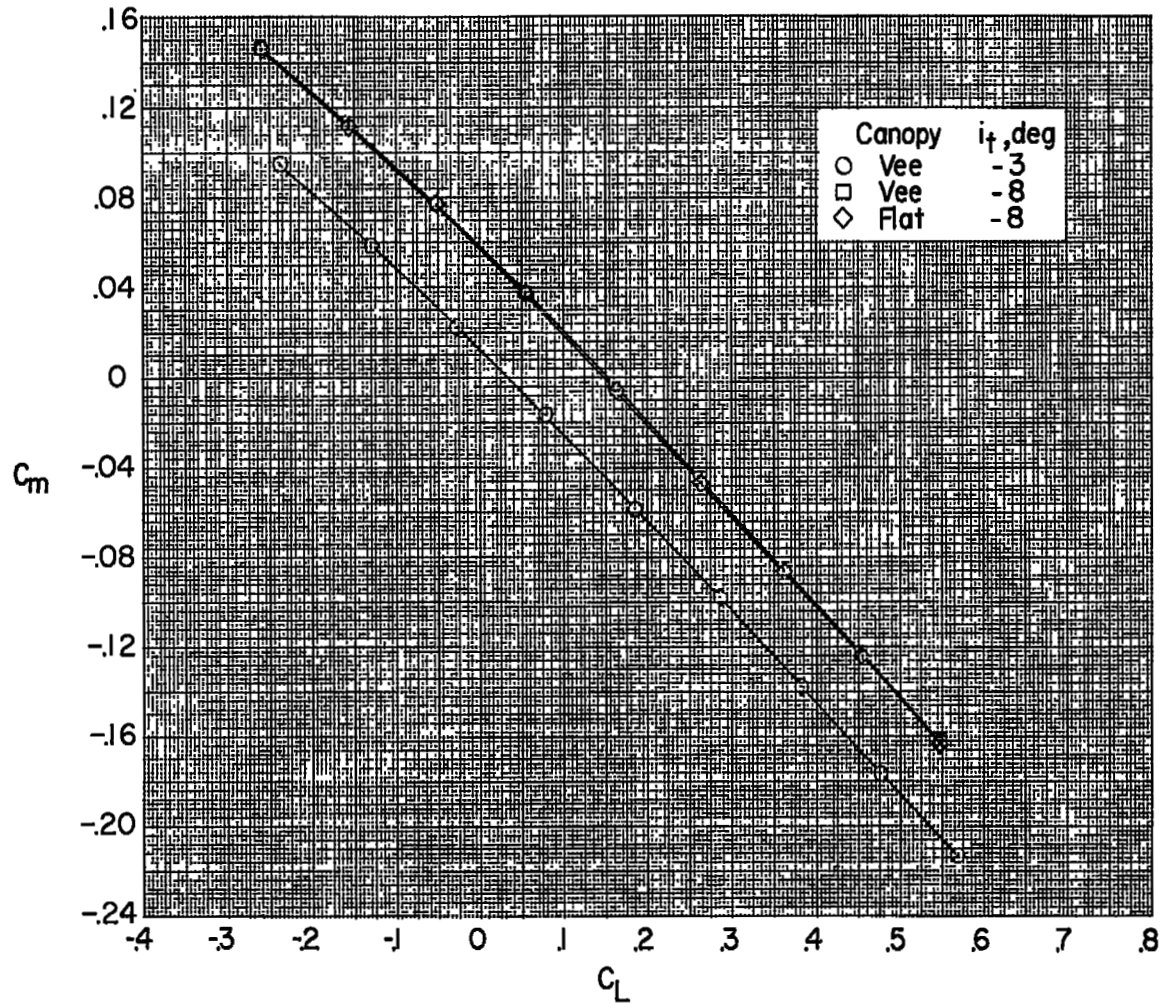
(b) Variation of pitching-moment coefficient with lift coefficient.

Figure 11.- Concluded.



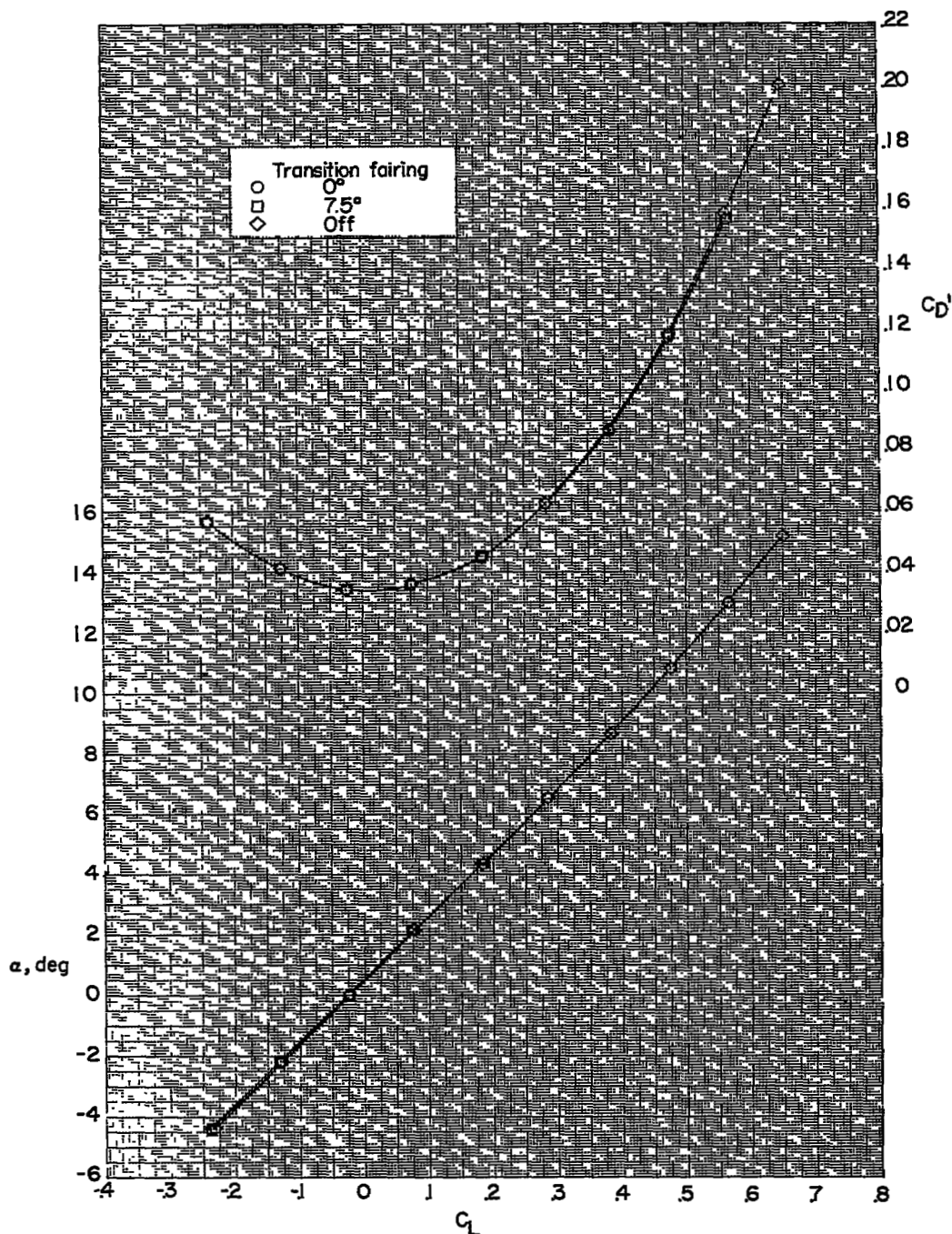
(a) Variation of drag coefficient and angle of attack with lift coefficient.

Figure 12.- Effect of canopy shape and horizontal tail deflection on aerodynamic characteristics in pitch. Basic nose; bump off; drooped inlet with 0° fairing; $A = 3.2$.



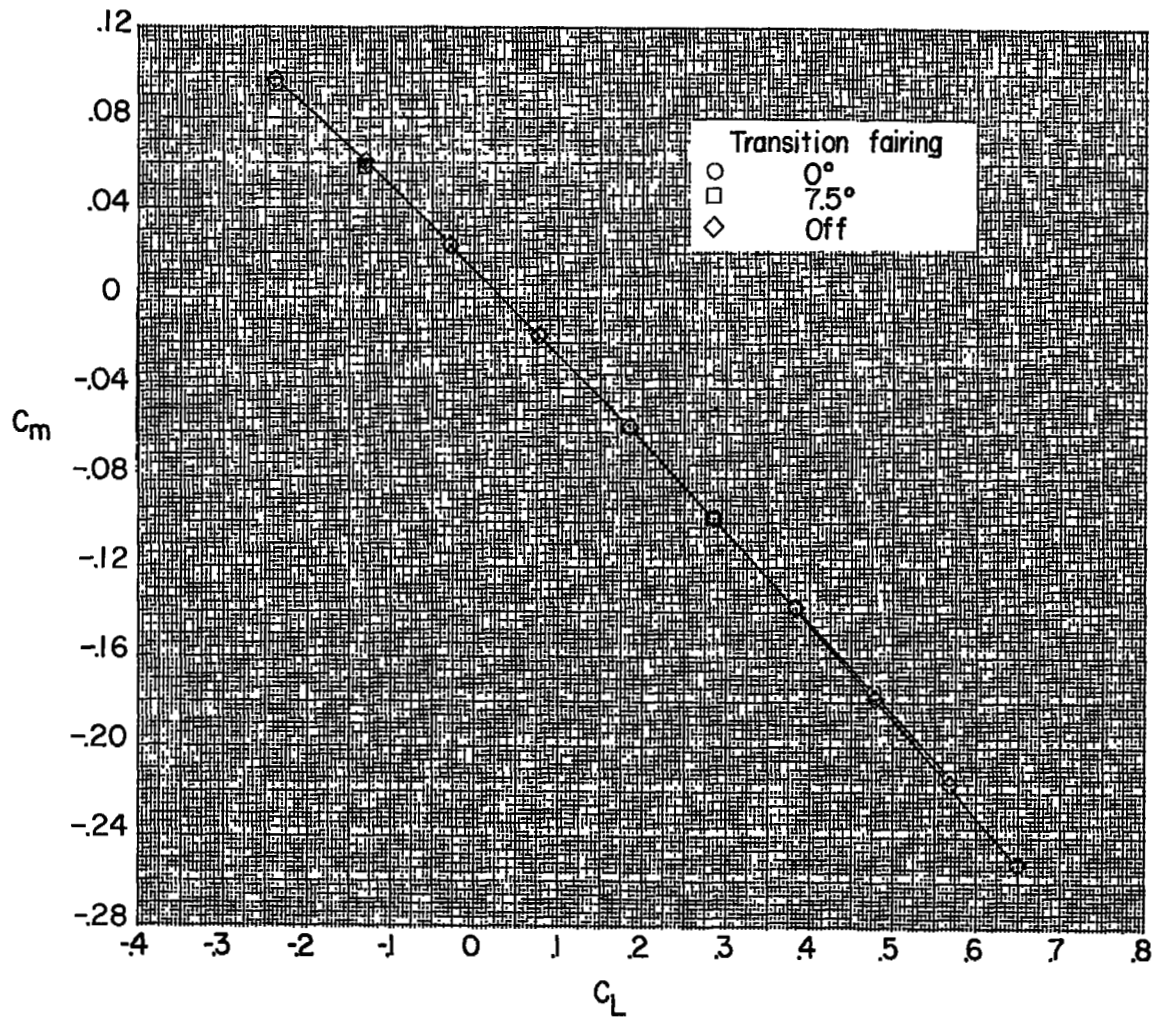
(b) Variation of pitching-moment coefficient with lift coefficient.

Figure 12.- Concluded.



(a) Variation of drag coefficient and angle of attack with lift coefficient.

Figure 13.- Effect of inlet transition fairing on aerodynamic characteristics in pitch. Basic nose; bump off; $A = 3.2$; $i_t = -3^\circ$.



(b) Variation of pitching-moment coefficient with lift coefficient.

Figure 13.- Concluded.

~~UNCLASSIFIED~~
~~CONFIDENTIAL~~



Author	
Title	
Source	
Notes	
Accession	
Classification	
Availability	
Restrictions	
Other	

~~CONFIDENTIAL~~
UNCLASSIFIED